Manuscript Number:

Title: Numerical Analysis in the Design of Umbrella Arch Systems

Article Type: Full Length Article

Keywords: Forepole; Umbrella Arch; Numerical Modelling; Tunnel Design; Numerical Analysis

Corresponding Author: Mr. Jeffrey Oke, Ph.D (Candidate)

Corresponding Author's Institution: GeoEngineering Centre, Queen's-RMC

First Author: Jeffrey Oke, Ph.D (Candidate)

Order of Authors: Jeffrey Oke, Ph.D (Candidate); Nicholas Vlachopoulos, BASc, MASc, rmc, PhD; Mark S Diederichs, BASc, MASc, PhD

Abstract: Due to advances in numerical modelling, it is possible to capture complex support-ground interaction in two-dimensions (2D) and three-dimensions (3D) for use in the analysis and design of complex tunnel support systems. One such system is the forepole element, installed within the umbrella arch temporary support system for tunnels which warrant such support measures. A review of engineering literature illustrates that a lack of design standards exists regarding the use of forepole elements. Therefore, when designing for such support, designers must employ numerical modelling and utilize engineering judgement. With reference to past developments by others and new investigation conducted by the authors on the Driskos tunnel and Istanbul Metro, this paper illustrates how advanced numerical modelling tools can facilitate understanding of the influences of design parameters associated with the use of forepole elements. In addition, this paper highlights the complexity of the ground-support interaction when simulated within 2D finite element software, using a homogenous reinforced region, and 3D finite difference software using structural elements. This paper further illustrates sequentially optimization of two design parameters (spacing and overlap) though the use of numerical modelling. With regard to capturing the failure region between the forepole support elements (spacing parameter), this paper provides examples of simplified and more advanced numerical methods and models. With regard to capturing behaviour, this paper employs three distinctive advanced numerical models: particle codes, such continuous finite element models with joint sets or voronoi blocks. And finally, with regard to capturing the behaviour/failure ahead of the tunnel face (overlap parameter), this paper employs two-dimensional axisymmetric models. This paper concludes with a 2D and 3D dimensional numerical assessment of the Driskos tunnel. The data rich case study is examined to determine an optimum design, based on the proposed optimization of design parameters, of forepole elements related to the site-specific considerations.

Suggested Reviewers: Daniele Peila
Associated Professor, Politechico di Torino
daniele.peila@polito.it
Dr. Daniele Peila, is an expert in this field. He hold numerous publications and has held short courses on the topic. One of his most recent short course on the topic took place before the world tunnelling conference in Switzerland (2013).

Grasso Piergiorgio
Geodata SpA
pgr@geodata.it
Mr. Piergiorgio Grasso is an expert in this field of monitoring and design of umbrella arch systems with numerous publications on the topic.

Quoc Nghia Trinh PhD
Research Scientist, SINTEF
Nghia.Quoc.Trinh@sintef.no
Dr. Quoc Nghia Trinh is an expert in the field of umbrella arch systems (Spiles) and has conducted many numerical analysis on this topic.

Jeffrey Oke
PhD Candidate, EIT
Queens-RMC Geo-Engineering Center

Bruce Wing/Miller Hall
36 Union Street
Queen's University
Kingston, Ontario
Canada, K7L 3N6
Phone: +1 613 217-8498
Fax +1 613 533-6592

26 June 2014

Editor-in-Chief Q.H. Qian
Journal of Rock Mechanics and Geotechnical Engineering
Tel. +86-27-8719 8182
Fax. +86-27-8719 9250
E-mail: rockgeotech@whrsm.ac.cn

Dr. Q.H. Qian

My co-authors and I, Jeffrey Oke, have been invited by Prof. Grasselli & Prof. Xia to submit our work to Journal of Rock Mechanics and Geotechnical Engineering in hope that it will be accepted and included to the special addition on "Advanced Numerical Methods in Rock Engineering". This work was presented at RockEng13 Symposium held in Toronto on December 6th, 2013 titled "Numerical Analysis in the Design of Umbrella Arch Systems".

Thank you for your time and considerations.

Jeffrey Oke

AUTHOR DECLARATION

We wish to confirm that that there are no known conflicts of interest associated with this publication and there has been no significant financial support for this work that could have influenced its outcome.

We confirm that the manuscript has been read and approved by all named authors and that there are no other persons who satisfied the criteria for authorship but are not listed. We further confirm that the order of authors listed in the manuscript has been approved by all of us.
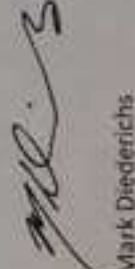
We confirm that we have given due consideration to the protection of intellectual property associated with this work and that there are no impediments to publication, including the timing of publication, with respect to intellectual property. In so doing we confirm that we have followed the regulations of our institutions concerning intellectual property.

We understand that the Corresponding Author is the sole contact for the Editorial process (including Editorial Manager and direct communications with the office). He is responsible for communicating with the other authors about progress, submissions of revisions and final approval of proofs. We confirm that we have provided a current, correct email address which is accessible by the Corresponding Author and which has been configured to accept email from jeffreyoke@gmail.com

Signed by all authors as follows:

Jeffrey Oke

Date: 30 June 2014

Nicholas Vlachopoulos

Date: 27 June 2014

Mark Diederichs

Date: 29 June 2014

To Whom It May Concern,

This letter is to confirm that the work contained in this manuscript has not been published previously as per the guidelines specified on your Journal's website and is not under consideration for publication elsewhere. Its publication has been approved by all relevant parties. If accepted, this work will not be published elsewhere.

Sincerely,

Jeffrey John

Date: 30 June 2014

Nicholas Vlachopoulos

Date: 27 June 2014

Mark Diederichs

Date: 29 June 2014

Numerical Analysis in the Design of Umbrella Arch Systems

Oke, J.[a] – jeffreyoke@gmail.com, (Corresponding author)

(Phone) +1 (613) 217-8498
(Fax) +1 (613) 533-6592
Bruce Wing/Miller Hall
36 Union Street
Queen's University
Kingston, Ontario
Canada, K7L 3N6

Vlachopoulos, N. [a] – vlachopoulos-n@rmc.ca

Diederichs, M.S. [a] – mdiederi@geol.queensu.ca

[a] GeoEngineering Centre, Queen's-RMC, K7L 3N6 , Kingston, Ontario, Canada

Abstract

Due to advances in numerical modelling, it is possible to capture complex support-ground interaction in two-dimensions (2D) and three-dimensions (3D) for use in the analysis and design of complex tunnel support systems. One such system is the forepole element, installed within the umbrella arch temporary support system for tunnels which warrant such support measures. A review of engineering literature illustrates that a lack of design standards exists regarding the use of forepole elements. Therefore, when designing for such support, designers must employ numerical modelling and utilize engineering judgement. With reference to past developments by others and new investigation conducted by the authors on the Driskos tunnel and Istanbul Metro, this paper illustrates how advanced numerical modelling tools can facilitate understanding of the influences of design parameters associated with the use of forepole elements. In addition, this paper highlights the complexity of the ground-support interaction when simulated within 2D finite element software, using a homogenous reinforced region, and 3D finite difference software using structural elements. This paper further illustrates sequentially optimization of two design parameters (spacing and overlap) though the use of numerical modelling. With regard to capturing the failure region between the forepole support elements (spacing parameter), this paper provides examples of simplified and more advanced numerical methods and models. With regard to capturing behaviour, this paper employs three distinctive advanced numerical models: particle codes, such continuous finite element models with joint sets or voronoi blocks. And finally, with regard

to capturing the behaviour/failure ahead of the tunnel face (overlap parameter), this paper employs two-dimensional axisymmetric models. This paper concludes with a 2D and 3D dimensional numerical assessment of the Driskos tunnel. The data rich case study is examined to determine an optimum design, based on the proposed optimization of design parameters, of forepole elements related to the site-specific considerations.

1. Introduction

As underground excavation designs become larger and more complex, numerical analysis is required to combat increasingly difficult ground conditions. In such conditions, reinforcement or strengthening is required prior to excavation, known as pre-support. Due to its time and cost effectiveness in comparison to other pre-support methods (ground freezing, jet grouted columns, or pipe jacking), the umbrella arch method is a pre-support method that is increasing in popularity (Volkmann and Schubert, 2007). Despite an increase in inclination towards this particular support system, an increase in comprehension of the interactions between the support system and the surrounding ground has not yet been established (Volkmann, 2003). Since 1991, literature has agreed that such limited understanding is due to lack of objective design criterion for the umbrella arch (Carrieri et al. 1991, Hoek 1999, Volkmann 2003, Kim et al. 2005, Volkmann et al. 2006, Volkmann and Schubert 2006 and 2007, Federal Highway Administration (FHA) 2009, Volkmann and Schubert 2010, Hun 2011, and Peila 2013). One explanation for this lack of design standard is that currently no set nomenclature for the method exists. Oke at al. (2014a) have attempted to address this issue by arranging the umbrella arch methods into thirteen sub-categories and associating them to applicable, specific failure mechanisms within the Umbrella Arch Selection Chart (UASC). This paper will focus on two of the sub–categories which employ the forepole element (confined and grouted in place) of the umbrella arch. This paper will further illustrate the use of numerical modelling with regard to the overall response of the umbrella arch with forepole elements and the optimization of select design parameters for a squeezing failure mechanism, as illustrated in Figure 2. The overall response investigation was conducted through the development of calibrated numerical models of two different tunneling projects with in-situ data: the Driskos tunnel project (Vlachopoulos 2009), and the Istanbul metro (Yasitli, 2012), further information on which will be presented in subsequent sections. Optimization of select design parameters was carried out for the severe squeezing ground at the Driskos tunnel at section 8+746 (Vlachopoulos and Diederichs, 2013.

Figure 1: Structural layout of the umbrella arch temporary support system with forepole elements. Red arrows and text indicate key design dimensions. A) Oblique support layout view displaying: L_{fp} = Length of forepole, and L_{fpo} = Length of forepole (or umbrella arch) overlap. B) viewport of "D" displaying: S_{cfp} = center to center spacing the forepole elements; t_{fp} = thickness of the forepole element; and ϕ_{fp} = outside diameter of the forepole element. C) Profile support layout view displaying: α_{fp} = installation angle of the forepole element; and L_{us} = length of the unsupported span. D) Cross-sectional view displaying: D_t = Diameter of the tunnel; and α_{fpa} = coverage angle of the forepole elements.

Figure 2: Applications of numerical analysis for the design parameters, illustrated in Figure 1, and overall response of forepole umbrella arch methods.

2. Background

The definition of the umbrella arch, according to Oke et al (2014a), is a pre-support installed from within the tunnel, prior to the first pass of excavation, above and around the crown of the tunnel face which can be made up of spiles (length smaller than the height of excavation), forepoles (length greater than the height of excavation), or grout elements. This paper focuses specifically on the forepole elements, which are part of the systemic temporary support system (e.g. shotcrete, steel sets, rockbolts, etc. as shown in Figure 1). However, prior to illustrating the extensive three-dimensional (3D) numerical analysis of forepole design, further detail is necessary with regard to the following aspects: a. the design parameters associated with the forepole umbrella arch; b. relevant, cited literature investigations that highlight important design considerations; and c. the use of two-dimensional (2D) numerical investigation and their shortfalls. These aspects will be explained in detail in the following sections.

3. Design Parameters

The design parameters for the forepole umbrella arch, shown in red within Figure 1, will each be investigated in order to illustrate their influence on the overall support response, unless noted otherwise. Figure 1A displays the length of forepole element (L_{fp}), and the length of forepole (or umbrella arch) overlap (L_{fpo}). The L_{fp} parameter cannot be optimized through numerical analysis as too many non-geomechanical factors governing the design exist. The L_{fp} depend on economic considerations, accuracy of drilling, accessibility of equipment and drillability of with respect to ground conditions. The L_{fpo} can be optimized through the use of relevant numerical modelling runs as the overlap is required to ensure stability of the system and ground response, as illustrated in Figure 2, which is further explained in subsequent sections. In order to be effective in the longitudinal direction, the embedding of the forepole element requires sufficient distance (length) past the disturbed ground tunnel face region. This embedment ensures that there will be sufficient longitudinal arching, which is the transfer of the stresses at the tunnel face to the support system (in front of the face) to the stable ground (ahead of the face), as illustrated in Figure 3B, which is explained further in subsequent sections.

Figure 3: Illustration of arching: A) Local arching (modified after Doi et al. 2009) B) Longitudinal arching and Radial arching.

Figure 1B illustrates the center to center spacing of the forepole elements (S_{cfp}), thickness of the forepole element (t_{fp}), and outside diameter of the forepole element (ϕ_{fp}). The maximum S_{cfp} is defined by the requirement of developing a local arching effect, as shown in Figure 3A (Volkmann and Schubert, 2007). This local arching can be analysed and captured within numerical models, as illustrated in the top portion of Figure 2. It is important to note that the FHA (2009) has commented on the occurrence of a common misjudgement of the longitudinal (over estimation) and radial effects (under estimation) of the forepole design. Thus, there is a requirement for analysis on both a local (arching between forepole elements) and a global (complete system response) scale. The size of the forepole element is defined by two parameters: the t_{fp}, and the ϕ_{fp}. Ultimately, these parameters will define the stiffness of the forepole as well as the loading area. This paper will illustrate that numerical modelling can be effective in determining an optimum size of the forepole elements within an Umbrella Arch arrangement. This optimum size, however, is further influenced by the installation equipment and the commercially standardized elements (pipes) available.

Figure 1C displays the installation angle (α_{fp}) of the forepole element and the length of the unsupported span (L_{us}). The α_{fp} for spile element application within umbrella arch methods can range from 5-40° as it is designed to lock in structural components or to ensure a certain thickness of grout barrier around the excavation. For forepole elements, however, the α_{fp} is defined by other temporary support elements (shotcrete and steel set thicknesses) as well as equipment clearances, to allow for the lowest angle possible. One must remember that the forepole elements and the Umbrella Arch support system are not employed in isolation and are used in conjunction with other support elements. The lowest possible angle of installation is deemed to be ideal as most cases result in failure of the ground material up to the forepole elements. When such failure occurs, a niche (or saw-tooth) profile is created, as shown in Figure 4. This niche profile results in an increased excavation size which consequently increases the requirement for more and/or larger other temporary support elements, neither of which is economical. The parameter L_{us} is typically defined by the steel set spacing, however, as the forepole elements are the only support resisting failure within the region (unless other pre-support measures are taken, such as core-reinforcement), it is also important to take tunnel face stability into consideration when deciding on the L_{us}.

Figure 4: Niche (saw-tooth) profile construction due to the installation of umbrella arch with forepole elements.

Figure 1D defines the coverage angle of the forepole elements (α_{fpa}). The tunnel diameter, D_t, is a design parameter that defines the difference between a forepole element and a spile element, as previously mentioned. The α_{fpa} is defined by the failure mechanism more than the mechanical response of the system. For gravity driven failures, the forepole elements only requires a α_{fpa} around the crown (~120°) of the excavation to protect the workers working underneath. For subsidence driven failure mechanisms, it is more common to employ 180° coverage above the face of the tunnel (as shown in Figure 1D). Similarly, Song et al. (2006) state that 120° is optimal for weathered rock and 180° for soil. For squeezing ground conditions, Hoek (2007) suggests an increase of the coverage angle from 120° to 180° for severe to very severe squeezing conditions, respectively.

4. Literature Investigation

The previous sections on design parameters stemmed from an in-depth literature investigation and past studies based primarily on empirical data. The following sections consist of noteworthy literature investigations, founded primarily on numerical modelling, that support the requirement for the numerical investigations conducted in this paper.

4.1. Volkmann

As a researcher, Volkmann is distinguishable as one of the few who has carried out laboratory, in-situ, and numerical analysis on the forepole element. Of the following, Volkmann can be credited with either commentary or analysis: number of the elements, cost comparison, size of the element (stiffness), L_{fp}, impact of in-situ measurement, disturbed ground foundation, L_{fpo}, and forepole installation methods. Due to the numerical focus of this paper, only the results of quantity, cost and size of the forepole elements will be further described.

Volkmann and Schubert (2006) carried out an analysis based on changing the number of forepole elements required in installation. It remains unclear from the publication if spacing of the structural elements was constant, however, results found a decrease in settlement with an increase of elements (0-30 elements). Furthermore, Volkmann and Schubert (2006) compared the analysis of 20 larger elements, and found that numerically, 30 pieces of 114.3 x 6.3 mm forepoles had similar effects of reducing face and maximum settlement when compared to 20 pieces of size 139.7 x 8.0 mm. The rational for such results is explained by the passive response of the support, which requires displacement in order to mobilize the support effects. An increase in stiffness of the support element requires less displacement to mobilize the support effects. Furthermore, Volkmann and Schubert (2006) suggested that 20 of the larger forepole elements would increase both time and cost effectiveness. Volkmann and Schubert (2006) analysis, however, did not take into consideration the local arching failure that could occur due to the increase of the spacing of forepole elements. The results of Volkmann and Schubert (2006) and the arching statements from FHA reinforce the importance of a design process that incorporates the local and global response of the system.

4.2.   Song et al. (2013)

Song et al. (2013) carried out a numerical and analytical analysis on a large-diameter steel-pipe-reinforced umbrella arching method. In their analysis, Song et al. (2013) investigated the following parameters: S_{cfp} ranging 40-60cm; the size (ϕ_{fp} only) of the forepole element ranging 60mm to 114.3mm; overburden ranging 10-40m; the α_{fpa} ranging 20°-180°; ground stiffness; as well as the lateral earth pressure coefficient, ranging 0.4-0.6. All of the aforementioned tests were compared to the factor of safety (FOS) for bending (b) and shear (s). It must be noted that the other supports simulated in this numerical model were not changed (i.e. the shotcrete thickness was constant), and the effect of failing to consider this will be explained in subsequent sections.

The results of the parametric analysis by Song et al. (2013) found the following: as the ϕ_{fp} increased, FOS_s and FOS_b also increased; as the overburden depth increased, FOS_s and FOS_b decreased and converged; as the S_{cfp} increased from 40cm to 60cm, FOS_s and FOS_b decreased; and as the Young's modulus of the ground decreased, FOS_s and FOS_b and also decreased. On the whole, the FOS_b was found to be more critical than FOS_s. The observations made by Song et al. (2013) suggest that FOS_b should be used as the primary indicator when evaluating the stability of the forepole elements.

4.3.   Kim et al. (2005)

Kim at al. (2005) numerically analyzed the effect of an umbrella arch when employed with forepole elements within a grout zone around the outside of the excavation. The forepole dimensions used in this study were 60.8mm in diameter, 3mm thickness, and 12m in length. They were installed with a S_{cfp} of 0.4m and had 6m of L_{fpo}, and the umbrella arch had 120° of α_{fpa}. The grout was simulated by multiplying the original ground deformation modulus by a factor of two. Kim et al. (2005) analysis consisted of a parametric analysis of five different materials ranging from weathered soil to soft rock. The analysis also consisted of changing the overburden of the tunnel excavation from 0.5 to 3.0 of the diameter of the

tunnel. When compared to instances that did not install the system, their results determined that a greater impact of reducing the surface settlement when employing the umbrella arch system in weaker ground condition (See Figure 5). Through a retrogressive analysis, their results further indicated that a prediction of surface and tunnel crown settlement is possible. However, their results did not agree with the surface settlement reduction plot found in the empirically driven UASC (Oke et al. 2014a) as shown in Figure 5. A comparison of the results from Kim et al. (2005) and the surface reduction plot of Oke et al. (2014a) illustrates two important factors. Firstly, a parametric analysis with numerical models must be calibrated to a case study to bring any validity to the work and, secondly, due to the complexity of the umbrella arch system, it can prove very challenging to model numerically. These factors will be addressed in subsequent sections of this paper.

Figure 5: Surface settlement reduction plot from the Umbrella Arch Selection Chart (Oke et al. 2014). Black Diamonds indicate the results found from Kim et al. (2005). Note: FpGUA Forepole Grouted Umbrella Arch, FpdGUA Double Forepole Grouted Umbrella Arch, FpGoUA Forepole Open Grouted Umbrella Arch, FpGcUA Forepole Continuous Grouted Umbrella Arch, FpGdcUA Forepole Double Continuous Grouted Umbrella Arch, GoUA Open Grouted Umbrella Arch, GcUA Continuous Grouted Umbrella Arch

5. Numerical Investigation

The authors of this paper have conducted 2D and 3D parametric analysis in order to illustrate the challenges of modeling forepole elements numerically. In each respective case, analysis was conducted by industry standard programs: 2D numerical analysis was carried out by employing Phase2 v7 (Rocscience, 2010) and v8 (Rocscience, 2013); and the 3D analyses were carried out by employing FLAC3D v4 (Itasca, 2009). These analyses also took into account deep and shallow tunnel excavations. The deep excavation was based off the parameters used in Vlachopoulos (2009) and Vlachopoulos et al. (2013) investigation of the Driskos tunnel of the Egnatia Odos highway in Greece. The parameters selected are from section 4.3 of the Driskos tunnel where forepoles were employed in squeezing ground conditions of fractured flysch material. Selected ground parameters can be found in Table 1. The parameters provided the authors the opportunity to create a numerical model with previously verified input parameters (matched to average in-situ tunnel convergence). In an effort to further increase computational time, however, the simulation was simplified to a single circular tunnel excavation (full face), unless noted otherwise. An additional deep numerical model was also created based on a hypothetical squeezing case (hydrostatic condition at depth). The relevant general ground parameters of the generic squeezing model can be found in Table 1. Further details and rational on these numerical models will be explained in subsequent sections.

Table 1: Parameters used for Numerical Analysis. Note: D_t = diameter of tunnel; H_e = height of excavation

Parameters	Project *(Vlachopoulos, 2009)* Driskos Tunnel	*(Yasitli 2012)* Istanbul Metro	*(Oke et al. 2014b)* Generic Squeezing
Shape	Circle	Horseshoe	Circle
D_t (or H_e)	10m	6.8m	10m
In-situ Stress (or Overburden)	100m	10.75m	3MPa
Excavated Material	Flysch (GSI 31)	Clay	Mudstone (GSI=20)
Hoek-Brown (m,s,a)	0.66,0.000468,0.52	-	0.345,0.0001, 0.544

Mohr-Coulomb (C,φ)	290kPa, 36°	20kPa, 33°	235kPa, 30.2°
Modulus of Elasticity (E_{rm})	1442.1MPa	38MPa	400MPa
Poisons Ratio	0.25	0.33	0.25

The shallow excavation runs performed were based on the in-situ surface settlement results and support design of the Istanbul Metro, as published in Yasitli (2012) and Ocak (2008). Two different sections of the Istanbul Metro had similar geological profiles and structural layouts. The major difference, however, was that while one section employed an umbrella arch system with forepoles, the other section did not. This difference allowed the authors to validate the support system for both scenarios, and instilled confidence that the parameters used to simulate the forepole element were realistic. The parameters used to simulate the ground condition for the Istanbul tunnel can be found within Table 1.

5.1.   Two Dimensional Numerical Investigation

Literature concurs that 2D numerical analysis does not and cannot accurately simulate the response of forepole elements within an umbrella arch (Volkmann and Schubert 2007, and Peila 2013). In order to illustrate this inability, the authors conducted a series of 2D analyses using Phase2 v7, a finite element numerical modelling program (Rocscience, 2010). Two types of analyses were constructed to simulate the forepole elements within an umbrella arch. This first was a homogenous model, suggested by Hoek (2001) as a crude approach (Figure 6A). The second was an "as built" model where the forepoles were simulated explicitly (Figure 6B). Figure 6A illustrates that the stresses appear to capture the radial aching effect around the outside of the homogenous region but the model is not able to capture the local arching between the structural elements. Furthermore, the homogenous model is not able to capture the longitudinal stress transfer. When modelled as an "as built", no additional resistance to the deformation is provided by the forepole as shown in Figure 6B and Figure 7. Figure 7 illustrates the convergence of the unsupported, homogenous, multiple "as built" simulated models and multiple 3D numerical model results. The homogenous model was the only simulation that was able to capture the expected reduction in the crown convergence when other support members are installed. Analysis of this model has found that while the homogenous model might capture empirical trends of reduction of the crown convergence, this method does not, however, capture the true mechanical longitudinal response of the umbrella arch. This is because when the forepole elements are installed without other supports, there is no significant reduction to the crown displacement, as denoted by the 3D analysis results (squares within Figure 7). Furthermore, Peila (2013) stated that it is difficult or impossible to define the improved ground conditions. The authors agree with Volkmann et al. (2006) that the only acceptable application of the homogenous model exists when grout is continuously connected around the outside of the excavation (with or without steel reinforcement). Despite considerations of this type of umbrella arch, however, it remains difficult or impossible to correctly select the accurate stress release action required (Peila 2013) to capture the 3D tunneling effect of the tunnel face, as explained in detail by Vlachopoulos and Diederichs (2014).

5.2. Three dimensional Numerical Investigation

As previously explained, the authors conducted parametric analysis based on two different case studies to aid in the design and understanding of the forepole structural element. Both case studies have been simplified to single excavations with a constant excavation profile (no niche profile). The authors understood that such changes would, in turn, change the response of the Driskos tunnel excavation; however, the material and structural properties were selected from a previously calibrated numerical model. The change of excavation process and tunnel profile would have minimal impact on the already calibrated input parameters. Further simplifications to the numerical models will be stated in the following sections. Still, the authors conducted a parametric analysis on the interaction parameters for the forepole structural elements in order to fully comprehend their influence before any parametric analysis took place. This parametric analysis on the interaction parameters will be discussed in the following sections. The numerical mesh and boundary conditions for this analysis of the Driskos tunnel can be found within Figure 8A-C.

The model setup for the Driskos tunnel has a boundary width of $9D_t$ from the center of the tunnel axis, and longitudinal boundary of $4.5D_t$ from the recorded data collected (Figure 8B). The normal direction boundary conditions are fixed at the bottom and at the entrance plane of the excavation sequence. The top middle strip of the model is also fixed in a direction parallel to the tunnel axis (Figure 8A and C). Stress conditions are applied on all remaining boundaries to simulate gravity loads (Figure 8A and C). The mesh was graded with a finer mesh (0.25m) at the center expanding to the peripheries. This primary numerical investigation of the Driskos tunnel simulated the forepole elements solely (no other support was simulated) in order to capture the independent influence of the support element, unless noted otherwise.

The numerical mesh applied for the analysis on the Istanbul Metro (Yasitli, 2012) can be found within Figure 8D, and had similar boundary distances and condition to the Driskos case except, the surface (top) boundary condition had an applied pressure of 100kPa to simulate the influence of building and traffic (Yasitli, 2012). The calibration of the Istanbul Metro case study, was based on in-situ surface settlement results, and was also simplified to a single bore excavation. The simplification of the single bore excavation would cause an error within the numerical model, as the second excavation would influence the first. To better understand this simplification, a simple 2D analysis was conducted. The authors utilized Phase2 v8 (Rocscience, 2013) for the analysis in order to verify the impact of the twin tunnel excavation. A percent difference of 10 was found between the single excavation and double excavation when the umbrella arch method was not employed., as illustrated in Oke et al. (2013a). The

calibration of the Istanbul tunnel, and the further parametric analysis that took place will be explained in greater detail in the subsequent sections.

5.2.1. Forepole Numerical Structure Element Investigation

FLAC3D v4 (Itasca, 2009) possesses three different types of structural elements which can all be employed to simulate the individual forepole elements. These existing structural elements are CableSel, BeamSel, and PileSel (Figure 9A). The CableSel element is capable of taking on axial loading only, and is not able to capture the longitudinal beading/stress transfer response of a forepole element. The BeamSel element is capable of taking on both axial and bending forces; essentially, the PileSel is the BeamSel element with the additional "rock-bolt logic". "Rock-bolt logic" allows for the ability of the support element to account for changes in confining stress around the reinforcement, strain-softening behavior of the material between the pile and the grid, and tensile rupture of the pile (Itasca, 2009). The slider constitutive model follows a Mohr-Coulomb failure criteria and the spring is defined by its stiffness parameter (Figure 9C). The authors of this paper have found that the PileSel is most suitable for the simulation of the forepole element, in concurrence with other authors (Trinh et al. 2007, Vlachopoulos and Diederichs 2013, and Volkmann and Schubert 2006) who have studied numerically the umbrella arch systems.

Figure 9: Illustration of the PileSel element from FLAC3D: A) beam-column element; B) nodal division; and C) interaction parameters. Illustration modified after Itasca 2009.

The concern that the PileSel element presents lies in the requirement that an exact value for the interaction parameters must be selected (especially that of the stiffness parameters, Figure 9C). Itasca (2009) suggests that these interaction parameters should be found from laboratory tests, yet, if laboratory testing of this nature is not possible, as is the case in most investigations, the stiffness parameters can be approximated by the method defined by St. John and Van Dillen (1983). A simplified version of the St. John and Van Dillen (1983) equation (Equation 1) has been established in order to provide a reasonable calculation for the stiffness parameter, according to Itasca (2009). In addition, this simplification has a one-tenth factor which helps to account for the relative displacement that occurs between the structural element and the borehole surface (the annulus), as illustrated in Figure 9B. The material properties regarding grout are not always provided, as is the case for the Istanbul Metro from Yasitli (2012) and the Driskos Tunnel from Vlachopoulos (2009). Therefore, Itasca (2009) suggests that the stiffness parameters be set to ten times the equivalent stiffness of the stiffest neighboring zone (Equation 2, with m value as 1), which will be the forepole element, as a general rule.

$$k = \frac{2\pi G}{10 \cdot \ln\left(1 + \frac{2t_a}{\varphi_{fp}}\right)} \tag{1}$$

$$k = 10^m \cdot E_f \tag{2}$$

Where:

G = Shear modulus of surrounding material (usually grout);

t_a = Thickness of the annulus;

ϕ_{fp} = Diameter of the pipe;

m = Stiffness multiplier; and,

E_f = Modulus of Elasticity for the Forepole element.

Identification of the correct stiffness parameter is essential. If the selected stiffness parameter is too low, the rock mass deforms past the support element without capturing the true interactions. Conversely, if the stiffness parameter is too high, numerical instability is a possibility. Numerical instability is the result of the failure criteria of the interaction connection (slider) constantly resulting in failure with any slight movement of the numerical mesh around the structural element. An example of this sensitivity can be found in Figure 10. Figure 10 shows the displacement profile of the complete forpole element with 2 m having been excavated at the front end of the support element. The ensuing results are from adjustments of the interaction parameter by a factor of ten for the generic squeezing numerical model, as previously described. The result illustrates that the greatest magnitude of deflection for this simulation was found when m=0 and the cohesion, C, parameter of the normal interaction direction was set to zero. When the value of m was increased or decreased (from m=0), the maximum deflection value decreased. Further investigation on all of the interaction parameters will be conducted in the subsequent section.

Figure 10: Parametric analysis of interaction stiffness parameter in order to determine the maximum displacement for a forepole element for the generic squeezing numerical model. Positive distance is within the excavated zone and negative distance is in the unexcavated zone of the tunnel profile. Note: C=cohesion, $k=E_f \cdot 10^m$, where E_f = 200GPa.

5.2.1.1. Interaction parameters

The interaction parameters for the forepole element of the Driskos tuunel were investigated in an effort to illustrate the sensitivity of each of the parameters, as shown in Table 2. The base model employed the parameters suggested by Itasca (2009) and lowest values (expect practically zero values) found in literature (Trinh 2006). The low values of the sensitivity analysis were based on a zero or practically zero value and the high values were based on highest values found in literature (Vlachopoulos 2009 for FLAC3D and Funatsu, et al. 2008 for Particle Flow Code, PFC, (Itasca, 2002)) or a multiplication of the base value. An illustration of the interaction parameters between the pile elements and the numerical mesh can be found within Figure 9C.

Table 2: Interaction parameters for the sensitivity analysis of the PileSel interaction parameters with the associated analysis run number. Note: references [a]Itasca (2009), [b]Vlachopoulos (2009), [c]Trinh (2006), and [d]Funatsu, et al. (2008). Nomenclature: C_s = Cohesion, shear direction, ϕ_s = Angle of Friction, shear direction, k_s = Stiffness, shear direction, C_n = Cohesion, normal direction, ϕ_n = Angle of Friction, normal direction, k_n = Stiffness, normal direction, g = gap, C = Cohesion (of ground material), ϕ_{fp} = Outside diameter of the forepole element, and ϕ = Friction Angle.

Interaction Parameters							
FLAC3D code	cs_scoh	cs_sfric	cs_sk	cs_ncoh	cs_nfric	cs_nk	cs_ngap
Symbol	C_s	ϕ_s	k_s	C_n	ϕ_n	k_n	g
Units	[F/L]	(degrees)	[F/L^2]	[F/L]	(degrees)	[F/L^2]	on/off
Base	[a] $C \cdot \phi_{fp} \cdot \pi$	[a] ϕ	[c]1.0E+07	[a] $C \cdot \phi_{fp} \cdot \pi$	[a] ϕ	[c]1.0E+09	off

	2C·ϕ_{fp}·π	2φ	[b]1.0E+11	2C·ϕ_{fp}·π	2φ	[d]1.0E+12	
High value	2C·ϕ_{fp}·π	2φ	[b]1.0E+11	2C·ϕ_{fp}·π	2φ	[d]1.0E+12	on
Low value	0	0	0	[c]0	0	0	
High Run#	RUN 1	RUN 3	RUN 5	RUN 7	RUN 9	RUN 11	Run 13
Low Run#	RUN 2	RUN 4	RUN 6	RUN 8	RUN 10	RUN 12	

The results of this sensitivity analysis are illustrated in Figure 11 and Figure 12. Figure 11 displays the results of the sensitivity analysis on the tunnel convergence recorded at the tunnel face and at three diameters of the tunnel away from the tunnel face ($3D_t$). The parameters which displayed an influence on the tunnel convergence in Figure 11 were plotted in Figure 12. Figure 12 displays the difference profile displacements that were captured in the sensitivity analysis. The most notable analyses from Figure 12 are run 12 and run 8. Run 12 had a practically zero value for the normal stiffness, k_n, value. Due to such a low k_n, little or no stress interaction occurred between the supports of the deforming ground. The results from run 12 suggests that the majority of mechanical response from the forepole element comes from the normal stress interaction. Run 8 illustrated that the interaction parameter failure occurred between the start of the forepole and the tunnel face, allowing the ground material to "flow" around the structural element. The results of this sensitivity analysis found that the k_n parameter will govern the deflection profile of the forepole element. Furthermore, the cohesion, C_s and shear stiffness, k_s, parameter are the second and third most influential parameter.

Figure 11: Percent difference of displacement from baseline interaction parameters values. Note: $3D_t$ denotes that the measurement of the convergence is taken 3 diameters of the tunnel distance away from the tunnel face. Interaction parameters for each Run # can be found in Table 2. (modified from Oke et al. 2012).

Figure 12: Displacement profile of first 3m of a 12m forepole element from numerical analysis with 1m of overhang. Runs that were too similar to base results were not shown in chart. Interaction parameters for each Run number can be found in Table 2.

The authors utilized the lessons gleaned from the interaction sensitivity analysis in order to calibrate the Istanbul Metro case study. In order to calibrate the numerical model, the k value (normal and shear) was adjusted for all structural elements in situations involving tunnels built without forepole elements. This situation was captured within 5% of the in-situ data, which is within acceptable limits of possible error due to the aforementioned simplification of the single tunnel excavation. The calibration of the model with the forepole element required an more intensive process as illustration Figure 13. Figure 13 illustrates the three step process carried out in order to find the greatest impact of reducing surface settlement due to the installation of the forepole element. First, the k_s and k_n multiplier, m, were increased (denoted by the black square in Figure 13) from 1 until it became evident that minimum surface settlement was present. This minimum value occurred when the stiffness multiplier was at 4. Next, the normal multiplier was held constant at m=4 while the k_s parameter was varied from 1 to 6, as denoted by the black diamonds in Figure 13. As is illustrated, there was no change to the ground surface settlement value until the k_s parameter multiplier reached greater than 4. In the third of three steps, the shear multiplier was held constant at m=4 while the k_n parameter was varied from 2 to 5, as denoted by the black triangles in Figure 13. The smallest amount of surface settlement was captured when the k_n multiplier was reduced to 3. Consideration of these results dictated that the forepole elements' shear and normal stiffness multiplier was set to 4 and 3, respectfully, for parametric analysis of the design

parameters for the Istanbul Metro. The calibrated numerical model with forepole elements was within 25% of the in-situ results; a difference of only 10mm. Such a marginal difference can be credited to an inaccurate capture of the interaction between the forepole element and other structural support members, as explained in the subsequent section.

Figure 13: Numerical results of the Istanbul Metro for calibration of the normal and shear stiffness interaction parameters.

Trinh et al. (2006) found that a fixed connection between the other supports and the spile elements could reduce the displacement ahead of the tunnel face by 80%, when compared to the un-fixed (free) numerical analysis. However, it remains the authors' opinion that a forepole embedded into shotcrete forms an elastic or plastic connection, not a fixed connection. To date, FLAC3D does not support multiple-layered interaction connection (Itasca 2009), which makes an elastic/plastic connection difficult to incorporate. In lieu of this, the authors felt that a free connection would most closely represent reality and yield conservative results, therefore the numerical results are within reason of the in-situ data.

5.2.2. Design Parameters Investigation

As previously discussed, a parametric investigation on the Driskos tunnel and Istanbul Metro was conducted in order to illustrate the influence of each design parameter: S_{cfp}, α_{fpa}, the size/stiffness of the forepole element, α_{fp}, L_{fpo}, and the effect of other supports and geometry.

5.2.2.1. Center to Center Spacing

Center to center spacing, S_{cfp}, of the forepole element of an umbrella arch was investigated by increasing the number of forepole elements that spanned a coverage angle of 180° from 3 to 157. Figure 14 illustrates the results of this analysis. An increase in the number of forepoles from 3 to 53 yields a displacement at the free end of the forepole of 18% difference (denoted by the diamond markers within the embedded chart of Figure 14). Despite this, there remains only a 5% difference of displacement when increasing from 53 to 157 (denoted by the square markers within the embedded chart of Figure 14). Therefore, the addition of more forepoles in an effort to control deformation past this threshold is, perhaps, not significantly advantageous when balanced against material and operational costs (as noted previously in the investigation of spacing by Volkmann and Schubert (2006)). It is important to note that the numerical model mesh size was 0.25m at the tunnel boundary, which is nearly equivalent to the S_{cfp} of the 63 forepoles. Thus, after 53 forepoles (~0.3m spacing), minimal impact is influenced by the mesh size of the numerical mode. Furthermore, as the numerical model used was a continuous model, failure that would most likely occur between the larger spacing elements was not captured, rendering the results of this numerical analysis applicable only for stable (at the tunnel face) squeezing ground conditions, such as the Driskos case.

Figure 14: Displacement profile of the first 2m of a forepole element based on 3D numerical analysis with the Driskos tunnel parameters. The plot illustrates the values of displacement of the free end of the forepole while varying the number of forepoles.

5.2.2.1.1. Spacing and Coverage

The S_{cfp} was further investigated by employing the numerical model based on the Istanbul Metro. A numerical analysis was carried out which investigated the center to center spacing of 26cm to 50cm while simultaneously changing the coverage angle from 90° to 200°. Twenty-four analysis were conducted to allow for a higher resolution of natural neighbor interpolation of data points with the ranges examined. The results of this analysis, found in Figure 15, illustrate significantly little difference in reduction of surface settlement with the effect of spacing. The analysis finds that the coverage angle has a greater influence than the spacing of the forepole element on the global response of the system. It is also apparent from raw data, however, that the 40cm spacing is capable of controlling settlement more effectively than spacing with an equivalent coverage angle of up to 160°, indicating an optimum spacing value. Once again, however, this analysis was unsuccessful at capturing the local failure between the support elements, and the interaction parameters were calibrated to a spacing of 40cm. These results were capable of capturing the stress redistribution caused by the installation of the forepole elements, illustrated within Figure 16. Figure 16 displays the final displacement of three different points around the tunnel cavity for varying coverage angles while maintaining constant spacing (40cm). The results found that the stresses are first redistributed to the side walls, causing great deformation. As the coverage angle increases, the stresses are transferred away and below the excavation, decreasing the convergence of the side walls further.

Figure 15: The effect of center to center spacing and coverage angle on surface settlement based on numerical models (24 parametric analysis) of the Istanbul Metro.

Figure 16: Effect of coverage angle on displacement for a 40cm forepole spacing for the Istanbul Metro analysis. Right embedded image displays a α_{fpa} of 200, and the arrow illustrate the location of referenced displacement to the respected colour.

5.2.2.2. Size/Stiffness of the Forepole Element

A parametric analysis based on the Driskos tunnel was also conducted on the size of the forepole element for the numerical model. The ϕ_{fp} were selected to capture the full range of acceptable forepole sizes. The smallest diameter was that of the largest standard size rebar used in Europe (50mm). The range of forepole metal pipes used in the analysis were values as cited in literature. Intermediate sizes were also evaluated in order to determine the effects of a constant t_{fp} (6.5mm) while simultaneously altering the ϕ_{fp}, and a constant ϕ_{fp} (141mm) while altering the t_{fp}. These numerical changes to the size of the forepole element, however, only affect the stresses being applied to the structural element (surface area) and the stiffness of the structural element. The purpose of these numerical runs was to try and determine the existence of an optimal range of forepole size. Forepole elements require a minimization of stress concentrations to ensure a large enough exposed perimeter to disperse stresses, but must be simultaneously small enough to move with the ground. The result of this analysis can be found within Figure 17. The optimum size for the ϕ_{fp} was 101-141mm, with a t_{fp} of 4-6.5mm, which resulted in a moment of inertia range of 2.2-6.2e6mm^{4} as denoted with black lines within Figure 17 as well as the squares within the imbedded image.

5.2.2.3. Angle of Installation

The angle of installation (α_{fp}) was also investigated using the Driskos tunnel numerical model. The change of the α_{fp} was adjusted by increasing the rise of the forepole element. The lowest rise was set to capture the extreme case whereby the forepoles were separated by 12cm (to allow for the application of shotcrete and other relevant support, and accessibility of equipment). The rise was increased slightly in order to capture the typical installation angles (between 3-7°). Further incremental runs were conducted until a rise of 3.6m was achieved, in an effort to capture an installation angle of greater than 15°. Such an analysis indicated that increasing the angle of forepole installation will decrease the displacement of the forepole. On average, the forepole also experiences 2.6 mm of displacement at the face. Conversely, a decrease in convergence is seen at the tunnel at the face (3.51%) and 3Dt from the face (2.82%) as the rise is increased from 0.4 to 3.6m. Within the forepole structural element itself, the numerical analysis captured a compression of 800N for 0.4m rise, which is in sharp contrast to a recorded tension of 4200N in the 3.6m rise. It can be postulated that with an increased angle, the forepole would act in a mode similar to that of a rockbolt rather than purely a forepole function. This conclusion is conducive with rockbolt design logic; usually most effective when installed normal to the tunnel axis and taking on tension, where forepoles take on compression axial force (Volkmann and Schubert 2007).

The niche profile is defined by the α_{fp}, which creates a greater excavation opening with a larger angle. This analysis did not, however, simulate the niche profile and as such, did not capture the effect of the increasing excavation opening size with the increasing α_{fp}. From the authors' collective experiences, the minimal improvement to convergence for the numerical model does not outweigh the potential for further convergences based on the absent assumptions of the numerical model. Thus, the authors conclude from this analysis that the α_{fp} of a forepole element should not diverge significantly from the horizontal plane unless structural analysis is conducted, in order to ensure that support is analysed in accordance with the various modes of failure. The results of this analysis can be found within Figure 18.

Figure 18: Displacement profile of first 2m of forepole from numerical analysis, based on the Driskos tunnel, of varying rise with 1m of overhang. The embedded plot illustrates the values of displacement of the free end of the forepole (modified from Oke et al. 2012b)

5.2.2.4. Overlap of Umbrella Arch

An investigation was carried out in order to determine the effect of overlap on the umbrella arch, (L_{fpo}) design for the Istanbul Metro. This analysis, however, was modified to a full face excavation in order to remove the influence of staged face excavation (i.e. top heading and bench) on the tunnel face and to promote more convergence at the tunnel face. An analysis was conducted for 0, 3, 4, 5, and 6m overlaps, as shown in Figure 19. Figure 19 illustrates the improving trend of the L_{fpo} when a. the density of the face reinforcement has been kept consistent with the original design and b. the face

reinforcement is not altered from the original design (support only installed within top heading region). In both cases, the trend regarding an improvement of the reduction of surface settlement converges when the L_{fpo} is greater than the Rankine block failure distance, RFD (i.e the distance away from the face that the RFD passes), as illustrated in Volkmann and Schubert (2010), Wang and Jia (2008), and Shin et al. (2008). This finding indicates that in order to optimize the umbrella arch effect on surface settlement, the L_{fpo} should always be installed just past the failure zone distance, ahead of the tunnel face. Furthermore, it was found when the umbrella arch was not installed, there was only a 13% improvement of the surface settlement by increasing the face reinforcement from (b) to (a). Comparably, when the umbrella arch was installed (3m of overlap only) there was an improvement of 58% to surface settlement when increasing the face reinforcement from (b) to (a), as shown in Figure 19. Such differences regarding surface settlement between the two face reinforcement patterns are caused by the redistribution of stresses at the invert of the tunnel, resulting in larger displacements at the bottom of the tunnel face. These results indicate the importance of well-designed face reinforcements and the requirement for further investigation of the impact of face reinforcement and umbrella arch interaction.

Figure 19: Effect of overlap on the Istanbul Metro with a full face excavation Note: (a) denotes constant soil reinforcement density used in the top heading of the original segmented excavation design; and (b) denotes soil reinforcement that was kept the same as the case study design (only employed in top heading). RFD = Rankine Block Failure Distance. FpGUA = Forepole Grouted Umbrella Arch. FpdGUA = double Forepole Grouted Umbrella Arch (modified from Oke et al. 2014c).

The effect of the overlap was also investigated with the generic squeezing numerical model. Two numerical analyses were carried out, the first with a 4m overlap and the second with 0m of overlap. The deflection profiles of the two numerical models are plotted in Figure 20 where 1m of the forepole element is only shown. The location of the free end of the forepole element was 2m from the tunnel face. The analytical models proposed by Oke et al. (2014b) were calibrated to the two different analysis by the least square analysis for both loading conditions defined by the longitudinal displacement profile (LDP) by Vlachopoulos and Diederichs (2009) and the modified LDP by Oke et al. (2013b). It was therefore determined that by curve fitting the deflection profile, a factor (0.5 and 0.4 for LDP and the modified LDP respectively) of the loading condition within the region of the overlap was required in order to match profiles. This is a promising result which captures the additional benefits of the overlap. However, additional investigation is required with regard to in-situ results in order to further quantify and validate this reduction of the loading condition. The analytical process is outside the scope of this paper, and will not be further discussed within this paper. For further explanation of this analytical process can be found in Oke et al. (2014b).

Figure 20: Results of numerical, based on the generic squeezing tunnel, and Semi-Analytical model, based on proposed model of Oke et al. (2014), overlap investigation. The 4m overlap case had a loading condition reduced by a factor of 0.5 and 0.4 for the LDP and modified LDP respectively.

5.2.2.5. Other Support Elements and Geometry

The impact of additional temporary support elements on the response of the umbrella arch support system has been determined to be critical. The empirical evidence used to create the UASC (Oke et al. 2014a) found that with increasing overburden there should be a greater reduction in surface settlement.

However, numerical models of the Istanbul Metro found that by changing the overburden by 2m there was an increase of 19% of surface settlement, as denoted by the 5 solid black outlined squared within Figure 21 (Oke et al. 2014c). This increase can be attributed to the 30% increase of the convergence of the excavation as the overburden increases and as the support system remained unchanged. Similar negative trend results with respect to overburden where also found when double Forepole Grouted Umbrella Arch, FpdGUA were investigated, as denoted by the 5 solid black outlined triangles within Figure 21. These results, as well as the results found from Kim et al. (2005), indicate that the design of the umbrella arch support required the inclusion of some type of factor associated with the remaining support system employed. Furthermore the results illustrate that the circle geometry creates less surface settlement (when umbrella arch is not installed) of 22% and 46% for the 6.5m, and 6.0m diameter tunnels, respectfully, when compared to the as built case for the Istanbul Metro. When an umbrella arch was installed for the 6.0m and 6.5m diameter tunnel, the reduction of surface settlement was found to be 53% and 58%, respectfully. Therefore, the circular tunnel diameter results found that, Forepole Grouted Umbrella arch, FpGUA, had less of an influence in reducing the surface settlement than when installed for a horseshoe profile. Similar results were found when FpdGUA, were installed in the Istanbul models, a 73% and 71% reduction of surface settlement occurred for the 6.5, and 6.0m diameter tunnels, respectfully.

Figure 21: Numerical Analysis results from the Istanbul Metro plotted on the subsidence management plot from the Umbrella Arch Selection Chart (UASC). Note: Squares denote analysis conduct with a FpGUA; and triangles denote a FpdGUA. Nomenclature:FpGdcUA = Forepole Grouted double continuous Umbrella Arch; FpGcUA = Forepole Grouted continuous Umbrella Arch; GcUA = continuous Grouted Umbrella Arch; and SEM = Sequential Excavation Method.

6. Optimization Methodology and Validation

Both the literature and the numerical investigations provide findings which support the inclusion of numerical assessment for the spacing and overlap design parameters in the umbrella arch system, prior to analysis of the global response. Such numerical assessments are required as these design parameters are based on local failure mechanisms which remain difficult to capture (and quantify) in a numerical analysis of the complete tunnel excavation. Within the following sections, the authors will propose an optimization methodology which employs numerical analysis for select design parameters. This optimization will be conceptually validated using the worst squeezing case scenario captured at the Driskos Tunnel at section 8+746. At this location, the FpGUA did not fail, so it is eligible as validation for the design methodology. The critical section, however, included displacements far greater than the average parameters used in previous analysis. Therefore, further investigation was required and will be present in the following section.

6.1. Driskos Twin Tunnel Construction Project

As previously stated, the preliminary properties conducted within this paper and used for the Driskos tunnel analyses, were found prior to the tunnel excavation. Upon excavation, it was discovered that at select locations the squeezing of ground material was far greater than anticipated (Vlachopoulos, 2009). The maximum recorded tunnel closure, during the top heading, was found to be 210mm (Egnatia Odos, 2001), along with primary support failures along a stretch of the left bore (Chainage 8 + 500 to 8 + 800)

(Grasso et al. 2005). From chainage 8+657 to 8+746 monitoring data was collected and presented within Vlachoupoulos (2009), as shown in Figure 22. The calibration process was carried out from the worst case of convergence from in-situ data, station 8+746. Despite the data existing as an isolated condition, the forepole elements did not fail, rendering the design recommendation functional for these conditions. While the preliminary properties successfully captured the trend of most of the in-situ data chainage 8+657, 8+697, 8+724, as illustrated in Figure 22, they underestimated the isolated condition displacement at chainage 8+746, despite the numerical model not having included any support elements. A back analysis conducted by Marinos et al. (2006) on a similar rock mass found that the σ_{ci} value was greatly overestimated for this isolated case, and must be reduced from 26.25 to 5-6 MPa for the given Driskos overburden. The reduction of rock mass parameters can be found within Table 3. This reduction allowed for displacements of an unsupported analysis far greater than the in-situ supported data results, as shown in Figure 22. The authors have conducted a calibrated as-built numerical model simulation of the Driskos tunnel section 8+746, as shown in Figure 23. The spacing and overlap design parameters, however, are the only parameters altered within this investigation; complete optimization for the other design parameters (ϕ_{fp} =101mm, t_{fp}=6.3mm, L_{fp} =12m, α_{fpa}=160° and α_{fp} =5.73°) will not be conducted. It is important to note, that the zero reading for the in-situ data was not taken till at least 10m back from the tunnel face, making it impossible to calibrate the numerical model to any displacement near the tunnel face.

Figure 22: Comparison of in-situ data to unsupported numerical analysis. Hollow markers denoted typical recorded data and filled markers denote the isolated squeezing condition. The grey shaded region represents the range of possible supported solutions based on numerical parametric analysis on the isolated ground material found in Table 3.

Figure 23: Illustration of the numerical model and support layout of the Driskos tunnel. A) Cross section image of the Numerical model of the Driskos tunnel. B) Support layout used at the Driskos tunnel project (Egnatia Odos AE, 1999). C) oblique image of the as-built design of Driskos tunnel with visual support element used for analysis, top heading only is excavated.

Table 3: Parameters used for the as-built Driskos Tunnel Numerical Analysis. Note: H_e = height of excavation

Project Parameters	Vlachopoulos, (2009) Marinos et al. (2006) Driskos 8+746
Shape	Horse Shoe
H_e (top/total)	8.78/11.70m
In-situ Stress (or Overburden)	106m
Excavated Material	Flysch (GSI 22)
Hoek-Brown (m,s,a)	0.478,0.000172,0.538
Mohr-Coulomb (C,φ)	118kPa, 21.3°
Modulus of Elasticity (rm)	681.1Mpa
Poisons Ratio	0.25

6.2.   Spacing Assessment

As previously mentioned, an investigation is required in order to capture the maximum spacing for the forepole elements within the Umbrella Arch arrangement. Otani et al. (2008) proposed experimental

design spacing based on the diameter of the forepole and the ground material friction angle. The result of this experimental design criterion theatrically maximizes the height of the failure region to the radius of the forepole. This design, however, does not take into consideration the effect of cohesion. The assessment from Doi and al. (2009) found that friction angle had minimal impact on the failure when compared to the cohesion parameter. In order to assess the possible maximum spacing, Doi et al. (2009) performed a trap door test using a discrete particle element model, PFC (Figure 3A and Figure 24A). Doi et al. (2009) employed the forepole elements as rigid (fixed) particles and sequentially removed the boundary condition between and underneath the elements. As previously stated, Doi et al. (2009) captured the effect of cohesion and friction angle, which was then related to the local failure height between the forepole elements. This height, however, was not associated with any design standard to replace the work of Otani et al. (2008).

Figure 24: PFC numerical Modelling of forepole spacing. A) Illustration of boundary arching effect of the ground caused from the imposed boundary conditions, modified after Doi et al. (2009). B) Illustration of local arching and failures, modified after Stockl (2002).

Based on the work of Stockl (2002), shown in Figure 24B, Volkmann and Schubert (2007) indicate that the required spacing was designed to maintain local arching. In this event, the heights of failure should not be an indication of the spacing design parameter, but instead be based on the forepole spacing ability, to prevent ravelling type failure mechanism between forepole elements. This type of failure mechanism could not be captured in Doi et al. (2009) analysis as the boundary conditions were not located in the center of the forepole element. Doi et al. (2009) boundary conditions impose a mirror on the outside edge of the model, resulting in the simulation of forepole elements with irregular spacing (side by side, space, side by side). This irregular spacing further results in a boundary arching effect, as shown in Figure 24A.

Stockl (2002) performed a small scale physical experiment to illustrate the two failure modes, local and global (Figure 25). Stockl (2002) illustrated that both of these failure modes could be captured within a comparable PFC numerical analysis (Figure 24A). The authors decided to therefore illustrate this method through the creation of a similar type of analysis geared toward discovery of the optimum forepole spacing. Two such methods are illustrated within this paper, the first a simplified model (continuum) while the second is an advanced model, such as the one proposed by Doi et al. (2009) and Stockl (2002).

Figure 25: Physical testing results of Stockl (2002). A: local failure between forepole elements. B: Global Arching failure across forepole elements.

6.2.1. Simplified Model

The simplified model will be illustrated by employing the Phase2 modelling program, based on a homogenous material, for the ground and element zones to represent the grout and forepole element. The boundary conditions and mesh of the simplified model are illustrated within the top portion of Figure 26, which also illustrates the resulting options for loading conditions. A constant field stress approach is one such option which captures the failure region as the stress concentration builds between the forepole elements, as the bottom boundary stress condition (p_i) is lowered from in-situ to zero. A second option employs gravity to define the boundary conditions. This option captures the stress

concentration as it builds atop the forepole elements, as well as the failure at the tunnel boundary surface, as the pressure is reduced. When compared with Stockl's (2002) calibrated numerical results, the gravity driven stress condition represents reality more accurately due to the shear failure developed above the forepole elements. The overall results, however, tend to develop a comparable tension failure region once the bottom pressure boundary is completely removed. Furthermore, the Phase2 analysis is a continuum model, and the ground material cannot fall between the forepole elements, as illustrated in the model by Doi et al. (2009). Based on the rigidity of the forepole elements and the imposed boundary conditions, a local arching effect will be consistently achieved (within realistic spacing parameters). The model, however, is capable of capturing the tension failure region, which, in theory, would have fallen out during the excavation sequence. Following the guidelines of Otani et al. (2008), if the maximum failure height is defined by the radius of the forepole element, then it is possible to employ this type of simplified numerical model in order to capture this failure height, with either field stress or gravity driven stress conditions.

Figure 26: Illustration of the simplified spacing assessment for a 114mm diameter forepole elements with 50cm spacing: Top – mesh and boundary conditions of numerical model; Middle – field stress driven failure region propagation; and Bottom – gravity driven failure region.

An analysis was conducted on the spacing based on the average Driskos tunnel parameters. The tension failure region was found to be greater than the radius of the forepole elements when spacing is increased to 35cm. These results agree with the as-built design of an initial spacing of 30cm for the forepole elements. The spacing of the forepole element, however, is not constant due to the angle of installation of the forepole elements. The forepoles at the Driskos tunnel project were installed at an angle of 5.73° which would result in a spacing of 36cm after 8m of excavation (the location of the next installation of forepole elements). An even greater spacing allowance could exist (44cm) if the calculation included the 0.5% average deviation of drilling (Mager and Mocivnik, 2000). Therefore, as an alternative to Otani et al. (2008), the authors hypothesize that a more appropriate design standard would designate that the maximum design spacing of the forepole element be based on the failure region height, equalling the diameter of the forepole element, as was found to be the average in the Driskos tunnel case.

Figure 27: Spacing assessment based on a 12m length of forepole element, with a α_{fp} of 5.73°.

6.2.1.1. Spacing: Driskos section 8+746

To further validate this failure region height, an analysis was carried out using the new properties for section 8+746 of the Driskos tunnel. It was concluded that the spacing could not be determined without taking into consideration the other support members and the effect of the tunnel face. The support pressure (bottom boundary condition) was reduced to the mobilized support pressure (0.32Mpa) based on convergence-confinement theory (Carranza-Torres 2004, Hoek 2007, Vlachopoulos and Diederichs 2009). It was found through the simplification model which maintains that a local failure between the forepole elements would occur between a spacing of 40cm to 45cm, as shown in Figure 28. This value is in agreement as the theoretical maximum spacing that occurred within section 8+746 was 44cm due to a 0.5% installation deviation and installation angle of 5.73°.

6.2.2. Advanced Models

The previous results may prove successful for homogenous materials, but may not be applicable for more complex material models where stability of the ground structure may be the governing factor (gravity driven failures). It is important to note that all of the further analysis of the spacing assessment will be performed with 50cm of spacing in order to promote the various failure modes that potentially could be exhibited by advanced numerical models.

While advanced models are capable of capturing the structural failure mechanism, the models do require calibration of the material parameters. Such calibration can be performed with the ground material simulated as a particle or discrete element model, or continuum (such as Phase2) model with simulated joints or voronoi grains. Calibration is required to ensure proper interaction between particles or joints, as shown in Potyondy and Cundall (2004) for PFC models.

As an alternative to discrete particle codes, Figure 29 provides an illustration of a voronoi model and displays three of the four different automatic voronoi mesh generations built into Phase2. The interaction parameters and the average size of the voronoi were held constant between the three different models, while the coefficient of uniformity was altered. It is apparent that the coefficient of uniformity has an additional impact on the design of the optimum forepole spacing, and should be taken into consideration for design. This voronoi process can also be easily simulated with discrete element models.

Figure 29: Illustration of the use of voronoi model to define the failure region for a 50cm forepole spacing with gravity driven stress condition. The red lines indicate the failure joint surface of the voronoi mesh.

When assessing the spacing of the forepole element, another aspect which must be taken into consideration during the design process is the joint network of the ground material. An illustration of the impact of the joints on the response of the spacing can be found within Figure 30. The left side of Figure 30 illustrates a hypothetical condition in which joints are offset by 90° but remain parallel and perpidicular to the tunnel boundary surface, respectfully. The right side of Figure 30 illustrates a hypothetical condition where joints remain offset by 90° but are 45° from the tunnel boundary surface. It is apparent in the right side that if the numerical model was not constrained within a continuum approach, a triangular shape block would have failed between the two forepole elements until the "apparent arch" was formed. Similarly, on the left side a possible rectangular block would have failed between the two forepole elements. With regard to the failure limit, however, it is not clear where the rectangular block failing would have propogated to. This joint model process could be easily simulated with UDEC, but is not illustrated within this paper.

Figure 30: Illustration of impact of joint sets on forepole spacing, modelled with gravity driven stress conditions. The red lines indicate that failure has occurred on the joint.

Though relatively simple, these advanced models can provide great insight into the mechanical interaction which exists between the individual forepole elements and the ground. Due to the demands regarding time, this type of assessment is not economically feasible (time requirement) within a complete 3D numerical analysis of the tunnel excavation. All other parameters, however, are capable of assessment in terms of the global response of the umbrella arch system, such as the overlap of the forepole elements.

6.3.   Overlap Assessment

As previously illustrated, the forepole element must be embedded past the disturbed zone ahead of the tunnel face. Within the numerical investigation of the Istanbul Metro, the Rankine active failure block was a suitable approximation of the required overlap of the forepole elements of the umbrella arch. The approximation, however, does not include the impact of other face stabilizing techniques. Limit equilibrium analysis could be taken into account for the other stabilizing techniques. This type of analysis is outside the scope of this paper, but will be investigated in future research. Another approach available for assessment of the overlap requirement is the axisymmetric analysis as it requires mere hours for capture, as opposed to days for a complete 3D numerical analysis. This axisymmetric analysis must be used with caution, however, as it is only truly applicable for installation of the forepole element in squeezing ground condition.

6.3.1. Axisymmetric Analysis

Axisymmetric analysis can be performed to illustrate the required overlap by assessing the distance from the tunnel face, along the tunnel boundary, to the outer limits of shear strain failure or the extent of plastic failure. An illustration of the extent of plastic failure can be found within Figure 31. The additional face stabilizing techniques can be simulated within the numerical analysis to capture their effect on the reduction of the required overlap. Structural supports within Phase2 analysis, however, cannot be simulated within axisymmetric analysis (except liners). Therefore, simplifications and/or approximations must be taken into consideration to simulate the face stabilizing techniques. To illustrate simplifications and/or approximations, the authors have conducted an assessment on face reinforcement (soil nails) simulated as internal pressure acting at the face and improved ground conditions (Figure 31). As is illustrated from the numerical analysis results presented in Figure 31, the support (shotcrete only) is capable of reducing the failure region ahead of the tunnel face. It is also apparent that face support (simulated by an applied pressure or improved ground condition) will further reduce the failure in the vicinity of the tunnel face. Therefore, before embarking on a time consuming 3D numerical analysis, a simple axisymmetric model can be substituted to find the failure region ahead of the tunnel face and to help define the overlap required of successive umbrella arches.

Figure 31: Illustration of the impact of different support (and simulation of support) on the distance to shear failure distance from the tunnel face along the excavation profile boundary.

6.3.1.1. Overlap: Driskos section 8+746

The requirement for overlap for a squeezing ground condition is completely different to that of a subsidence driven condition. To ensure optimal use of the support in terms of reducing surface settlement, subsidence requires that the next umbrella arch of support is installed while the embedded end of the current umbrella is in stable ground. In squeezing ground conditions the plasticity zone is fair greater, and it remains impractical to install an overlap with this guideline. Furthermore, the rationale for installing forepoles for squeezing ground conditions is to transfer the stresses longitudinally away from the tunnel face which will, in turn, reduce degradation of the rock mass through confinement. Therefore minimal embedment length, as opposed to subsidence, is required. From these considerations, the authors propose the selection of the overlap should be based on the maximum distances of the tension failure in front of the tunnel face. The required overlap, based on section 8+746, was found to be 1.488m for the unsupported analysis and 2.412m for the supported analysis, as shown in Figure 32. The design for the overlap, is also based on the pre-determined excavation steps, which was 2m. Therefore the optimum overlap should be 2m.

Figure 32: Tension failure of an axisymmetric analysis for the Driskos section 8+746. Left: unsupported, Right: supported (shotcrete only). Shear failure now shown within image.

6.4.   Driskos Tunnel Design Optimization

As previously stated in Section 6.1, without changing/optimizing the remaining design parameters, the results of the optimizing the initial spacing was found to be 25cm, based on a maximum spacing of 40cm with an a overlap of 2m for a 12m long forepole element, as previously illustrated in Figure 27. In an attempt to determine the optimal design, a comparison of the results from the as-built model and the improved design should be checked with a 3D analysis. As described by Song et al. (2013) the bending moment associated with the forepole support element will be the governing design parameter and will needs to be assessed for the optimization process.

Furthermore, an evaluation of the economic impact of this design change was conducted. For each umbrella arch installed, 10 more forepoles would need be employed to keep the same α_{fpa} when changing the initial spacing from 30cm to 25cm. This increase in forepole elements would require more time to install, slowing the excavation process. However, the decrease in the requirement for an L_{fpo} over a 40m stretch (before the next umbrella arch is installed) results in 1 fewer umbrella arch installation set up when changing the L_{fpo} from 4m to 2m. Ultimately this 1 fewer umbrella arch installation set up, which results in 10 fewer forepole elements total employed of 40m of excavation based on this optimization design. Therefore this optimization of design will decrease the time required to install by 10 fewer forepoles and 1 less set-up of the forepole jumbo for each 40m of excavation, increasing the excavation rate.

7. Summary and Conclusions

This paper has investigated relevant concepts with respect to the employment of numerical techniques and analysis in support of the design of umbrella arch systems. An examination of 2D numerical analysis

determined that such techniques were mechanistically incorrect in capturing the global response of such support systems, yet efficient at capturing localized failure between support elements and with respect to support-ground interaction; meanwhile, 3D analysis proved necessary for the capture of the global response of forepoles within an umbrella arch system. Through a detailed illustration of multiple, relevant sensitivity and parametric studies highlighted in the multiple sections of this paper, the importance of interaction parameters was emphasized, and procedures of recommended calibration processes were presented for both a shallow and deep tunneling excavation scenarios. The most sensitive parameters were determined to be k_n, k_s, and C_n. The individual influence of each respective design parameter on the global response was also presented.

The length of overlap, L_{fpo} was found to be related to the investigated failure region ahead of the tunnel face. For subsidence driven (shallow) designs, the L_{fpo} must be at a distance past the plastic failure region. For squeezing ground, the L_{fpo} must be at a distance past unstable ground conditions, with the extent of tension failure assumed. It was found that axisymmetric analysis was found to provide a quick approximation of this design parameter.

The coverage angle of the forepole elements, α_{fpa}, was found to exert a greater influence on the global response of a system when compared with the center to center spacing of the forepole elements, S_{cfp}. The S_{cfp} was found to be a critical design parameter, yet one that could not be easily captured in full scale, 3D numerical analysis. The authors have therefore proposed a 2D analysis approach in order to capture the maximum spacing, based on typical size/stiffness of the forepole elements (Diameter, ϕ_{fp} and thickness, t_{fp}), and installation angle α_{fp}. Such approaches can be employed for both squeezing ground conditions (continuum model) and gravity driven failure (particle, discrete, and jointed continuum models).

The increase of the angle of installation from the horizontal, α_{fp}, was found to slightly decrease the convergence of the continuous profile of the tunnel excavation. This result, however, proved to be relatively insignificant for a "saw-tooth" profile excavation due to the increased requirements of other support members. As noted previously, the umbrella arch with forepole elements is always employed in conjunction with other temporary support systems; these additional systems also have an influence on the global response of the complete system that must also be determined.

In conclusion, this paper presented the use of numerical techniques in order to add value to the understanding of the influences of design parameters on forepole elements used within an umbrella arch system. The paper also provided an overview of suggested, sound numerical modelling procedures for support systems, optimization of design, and the comprehensive performance of full 3D analysis on preliminary design.

It should be noted, however, that sound engineering judgement and a comprehensive understanding of the fundamentals associated with geotechnical, mechanistic and numerical analysis factors is always a prerequisite prior to conducting a preliminary design for tunnel construction of this nature. A designer must understand the limitations associated with the numerical tools combined with the accuracies

related to obtaining sound geotechnical data (i.e. input and interaction parameters, site-specific factors etc.).

8. Acknowledgement

9. References

Carrieri G, Grasso P, Mahtab A, Pelizza S. Ten years of experience in the use of umbrella-arch for tunneling. Int congress on Soil and Rock Improvement in Undergr Works 1991; 99-111.

Doi Y, Otani T, Shinji M. The Optimum Distance of Roof Umbrella Method for Soft Ground by Using PFC. In: Analysis of Discontinuous Deformation: New Developments and Applications, by Guowei Ma and Yingxin Zhou, 2009, Singapore: Research Publishing Services, 461-468.

Egnatia Odos A.E. Geological study by Asproudas and cooperates consultants (in Greek). 1998.

Egnatia Odos S.A. The Appropriate use of Geological Information in the design and construction of the Egnatia Motorway Tunnels, Tunnel Construction in Greece. Technical notes (Marinos and Hoek), Athens: Technical notes (MASc. program) of the National Technical University of Athens, Section 5, 2001.

Federal Highway Administration. Technical Manual for Design and Construction of Road Tunnels - Civil Elements. 1999. Available at: http://www.fhwa.dot.gov/Bridge/tunnel/pubs/nhi09010/errata.cfm (Date accessed 22 April 2014).

Funatsu T, Hoshino T, Sawae H, Shimizu N. Numerical analysis to better understand the mechanism of the effects of ground supports and reinforcements on the stability of tunnels using the distinct element method. Tunn and Undergr Space Technology Incorporating Trenchless Technology Res, 2008; 561-573.

Grasso P, Scotti G, Blasini G, Pescara M, Floria V, Kazilis N. Successful application of the observational design method to difficult tunnel conditions – Driskos Tunnel. In: Underground Space Use: Analysis of the Past and Lessons for the Future, 2005: 463-470.

Hoek E. Big tunnels in bad rock: 2000 Terzaghi lecture. ASCE Jour of Geotech and Geoenvironmental Eng, 2001: 726-740.

Hoek E. Support for very weak rock associated with faults and shear zones. International symposium of Rock and Support and Reinforcement Practice in Mining. Kalgoorlie, Australia , 1999.

Hun Y. Stability and collapse mechanism of unreinforced and forepole reinforced tunnel headings. National University of Sinapore, 2011. [Dissertation]

Itasca Consulting Group Inc. Fast Lagrangian Analysis of Continua in 3 Dimensions Version 4.0. Minneapolis: Itasca Consulting Group Inc., 2009.

Itasca Consulting Group Inc. Particle Flow Code, PFC v3.0. 2002.

Kim SH, Baek SH, Moon HK. A study on the reinforcement effect of Umbrella Arch Method and prediction of tunnel crown and surface settlement. In: Underground Space Use. Analysis of the Past and Lessons for the Future, by Yucel Erdem and Tulin Solak, 245-251. Istanbul: Taylor & Francis, 2005.

Mager W, Mocivnik J. Modern Casing Technology Sets a Milestone in Drilling and Ground Anchoring. Felsbau, 2000: 43.

Marinos V, Fortsakis P, Prountzopoulos G. Estimation of rock mass properties of heavily sheared flysch using. IAEG. The Geological Society of London, 2006. 1-12.

Oke J, Vlachopoulos N, Diederichs MS. Sensitivity Numerical Analysis of Orientations and Sizes of Forepoles for Underground Excavations in Weak Rock. In: 46th US Rock Mechanics / Geomechanics Symposium. Chicago: American Rock Mechanics Association, 2012b.

Oke J, Vlachopoulos N, Diederichs MS. Improved Input Parameters and Numerical Analysis Techniques for Temporary Support of Underground Excavations in Weak rock. In: RockEng. Edmonton, 2012a.

Oke J, Vlachopoulos N, Diederichs MS. Modification of the Supported Longitudinal Displacement Profile for Tunnel Face Convergence in Weak Rock." 47th US Rock Mechanics / Geomechanics Symposium. San Francisco: ARMA, American Rock Mechanics Association, 2013b.

Oke J, Vlachopoulos N, Diederichs MS. Semi-Analytical model of an Umbrella Arch Employed in Hydrostatic Tunnelling Conditions . In: 48th US Rock Mechanics / Geomechanics Symposium. Minneapolis: American Rock Mechanics Association, 2014b. 9.

Oke J, Vlachopoulos N, Diederichs MS. The Reduction of Surface Settlement by Employing Umbrella Arch Systems. GeoMontreal 2013. Montreal: Canadian Geotechnical Society, 2013a.

Oke J, Vlachopoulos N, Diederichs MS. The Reduction of Surface Settlement by Employing Umbrella Arch Systems for Different Excavation Methods. In: the ISRM European Rock Mechanics Symposium - EUROCK2014. Vigo: ISRM, 2014c.

Oke J, Vlachopoulos N, Marinos V. The Pre-Support Nomenclature and Support Selection Methodology for Temporary Support Systems within Weak Rock Masses. Geotech and Geol Eng 32, no. 1. 2014a: 97–130.

Otani T, Shinji M, Chijiwa T. Proposal of Numerical Model and the Determination Method of Design Parameters for Pipe Roofing Method. Daboku Gakkai Ronbunshuu 64, no. 4. 2008: 450-462.

Peila D. Forepoling Design. In Ground Improvement Pre Support & Reinforcement Short Course. Geneva: International Tunnelling and Underground Space Association (WTC 2013), 2013. [Lecture]

Potyondy DO, Cundall PA. A bonded-particle model for rock. Int J of Rock Mech and Min Sciences 41 2004; 1329–1364.

Rocscience Inc. Phase2 v7. Toronto, Ontario, 2010.

Rocscience Inc. Phase2 v8. Toronto, Ontario, 2013.

Shin JH, Choi YK, Kwon OY, Lee SD. Model testing for pipe-reinforced tunnel heading in a granular soil." Tunnelling and Underground Space Technology 23. 2008; 241-250.

Song KI, Cho GC, Chang SB, Lee IM. Beam–spring structural analysis for the design of a tunnel pre-reinforcement support system. Int J of Rock Mech and Min Sciences. 2013; 139-150.

St. John CM, Van Dillen DE. Rockbolts: A New Numerical Representation and Its Application in Tunnel Design. In: 24th U.S. Symposium on Rock Mechanics. College Station, Texas: New York: Association of Engineering Geologists. 1983; 13-26.

Stockl C. Numerische Berechnung der Tragwirkung von Rohrschirmen mit PFC-2d (In German). Graz: Graz University of Technology, 2002. [Dissertation]

Trinh QN. Analyses of a cave-in problem in a hydropower tunnel in Vietnam. Trondheim, Norway: Norwegian University of Science and Technology. 2006. [Dissertation]

Trinh QN, Broch E, Lu M. Three Dimensional Modelling of a Tunnel cave-in and spiling bolt support. In: Singapore: ISRM international Symposium 2006. 2006.

Vlachopoulos N, Diederichs MS, Marinos V, Marinos P. Tunnel behaviour associated with the weak Alpine rock masses of the Driskos Twin Tunnel system, Egnatia Odos Highway. an Geotech J. 2013; 91-120.

Vlachopoulos N. Back Analysis of a Tunnelling Case Study in Weak Rock of the alpine system in northern Greece: Validation and Optimization of Design Analysis Based on Ground Characterization and Numerical Simulation. Kingston, Ontario: Queens University, 2009. [Dissertation]

Vlachopoulos N, Diederichs MS. Appropriate Uses and Practical Limitations of 2D Numerical Analysis of Tunnels and Tunnel Support Response. Geotech and Geol Eng, 2014; 469-488.

Volkmann G. Rock Mass - Pipe Roof Support Interaction Measured by Chain Inclinometers at the Birgltunnel. In: International Symposium on Geotechnical Measurements and Modeling, Proc. . Karlsruhe: A.A. Balkema. 2003; 105-109.

Volkmann GM, Schubert W. A load and load transfer model for pipe umbrella support. Rock Mech in Civ and Environ Eng, 2010: 379-382.

Volkmann GM, Schubert W. Contribution to the Design of Tunnels with Pipe Roof Support. In: Asian Rock Mechanics Symposium. 2006.

Volkmann GM, Schubert W. Geotechnical Model for Pipe Roof Supports in Tunneling. In: Proceeding of the 33rd ITA-AITES World Tunneling Congress, Underground Space - the 4th Dimension of Metropolises. Prague: Taylor & Francis Group. 2007; 755-760.

Volkmann GM, Schubert W, Button EA. A Contribution to the Design of Tunnels Supported by a Pipe Roof. 41st U.S. Symposium on Rock Mechanics. Golden, Colorado, 2006.

Volkmann GM, Schubert W. Optimization of Excavation and Support in Pipe Roof Supported Tunnel Sections. In: ITA-AITES World Tunneling Congress. 2006; 404.

Wang H, Jia J. Analytical Method for Mechanical Behaviors of Pipe Roof Reinforcement. In: International Conference on Information Management, Innovation Management and Industrial Engineering. 2008. 353-357.

Yasitli NE. Numerical modeling of surface settlements at the transition zone excavated by New Austrian Tunneling Method and Umbrella Arch Method in weak rock. Saudi Society for Geosciences, 2012.

10. Nomenclature

Center to center spacing the forepole elements	S_{cfp}
Cohesion	C
Continuous Grouted Umbrella Arch	GcUA
Coverage angle of the forepole elements	α_{fpa}
Diameter of the tunnel	D_t
Double Forepole Grouted Umbrella Arch	FpdGUA
Factor of Safety: Bending	FOS_b
Factor of Safety: Shear	FOS_s
Federal Highway Administration	FHA
Forepole Continuous Grouted Umbrella Arch	FpGcUA
Forepole Double Continuous Grouted Umbrella Arch	FpGdcUA
Forepole Grouted Umbrella Arch	FpGUA
Forepole Open Grouted Umbrella Arch	FpGoUA
Friction Angle	ϕ
General stiffness parameter	K
Geological Strength Index	GSI
Height of excavation	H_e
Hoek-Brown a	a
Hoek-Brown m	m
Hoek-Brown s	s
Installation angle of the forepole element	α_{fp}
Intact rock mass strength	σ_{ci}
Interaction parameter: Angle of Friction, normal direction	ϕ_n
Interaction parameter: Angle of Friction, shear direction	ϕ_s
Interaction parameter: Cohesion, normal direction	C_n
Interaction parameter: Cohesion, shear direction	C_s
Interaction parameter: Stiffness, normal direction	k_n

Interaction parameter: Stiffness, shear direction	k_s
Length of forepole	L_{fp}
Length of forepole (or umbrella arch) overlap	L_{fpo}
Length of the unsupported span	L_{us}
Modulus of Elasticity of Rock Mass	E_{rm}
Modulus of Elasticity of the forepole element	E_f
Open Grouted Umbrella Arch	GoUA
Outside diameter of the forepole element	ϕ_{fp}
Particle Flow Code	PFC
Rankine Block Failure Distance	RFD
Reduction of Surface Settlement	Rss
Sequential Excavation Method	SEM
Shear modulus of surrounding material (usually grout)	G
Stiffness multiplier (variable)	M
Surface settlement with Normal Support	δ_{sNS}
Surface settlement with Normal Support with addition Umbrella Arch	δ_{sNS+UA}
Thickness of the annulus	t_a
Thickness of the forepole element	t_{fp}
Three-dimensions	3D
Two-dimensions	2D
Umbrella Arch Selection Chart	UASC

Figure1
Click here to download high resolution image
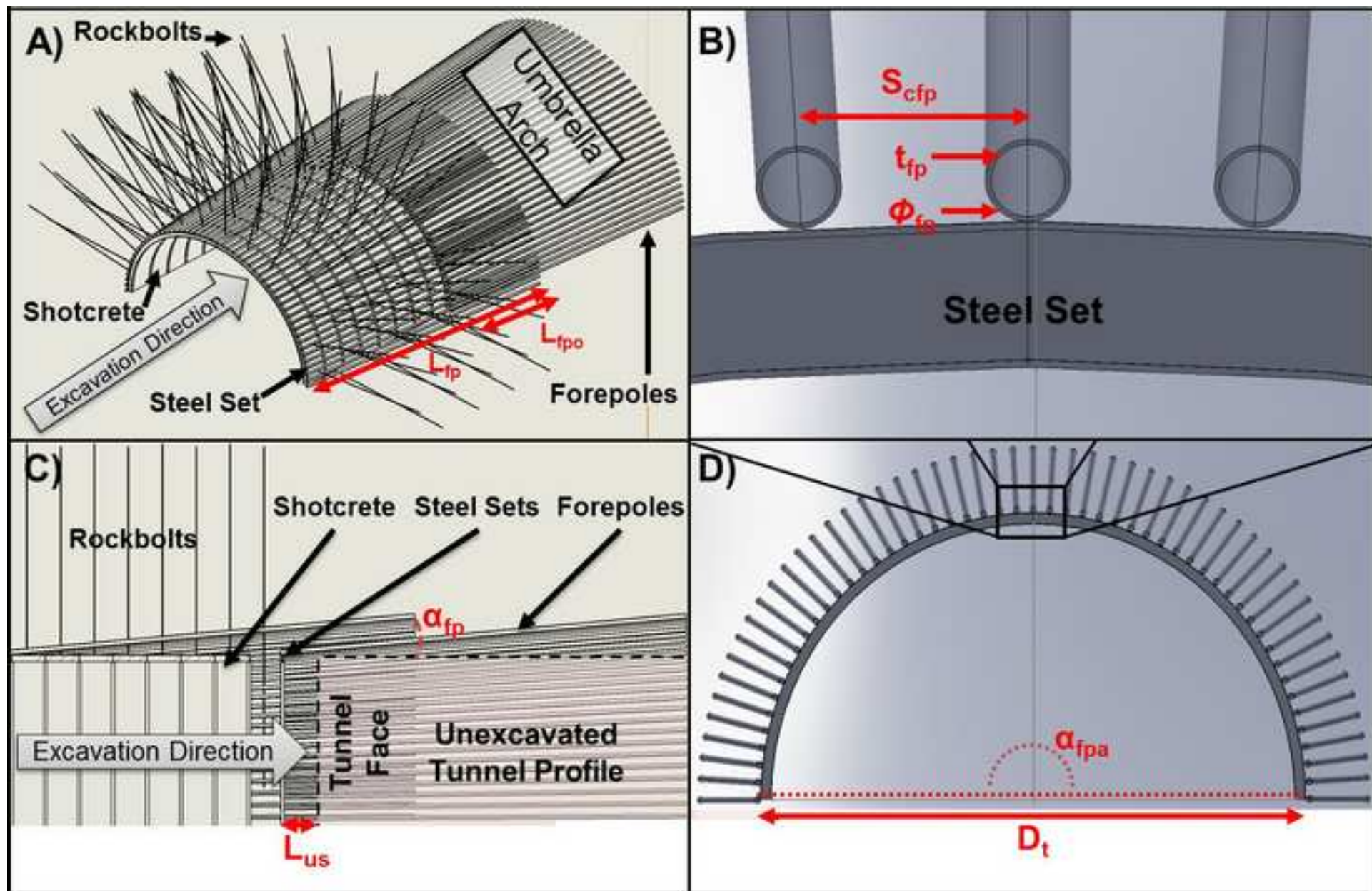
Figure2
Click here to download high resolution image
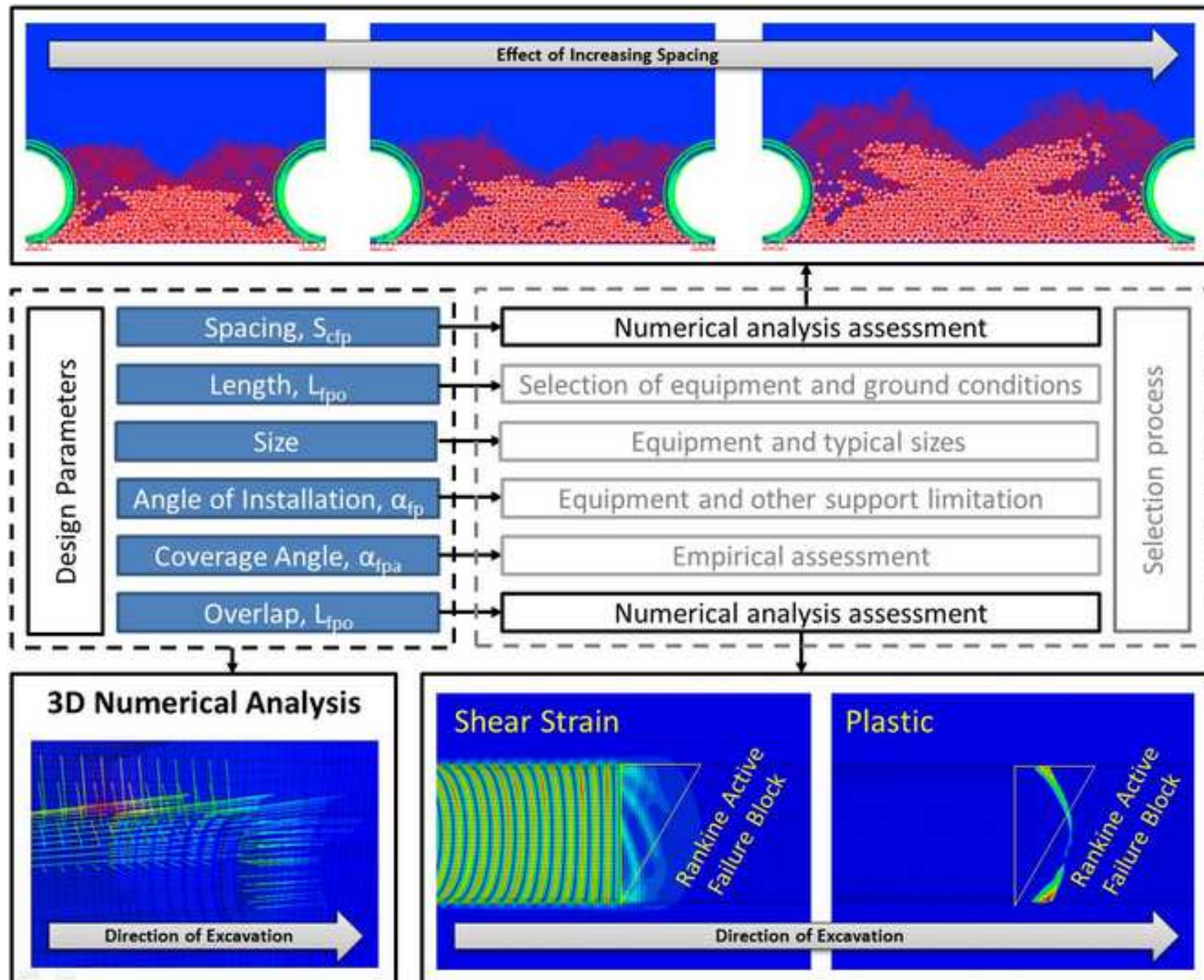
Figure2

Figure3
Click here to download high resolution image
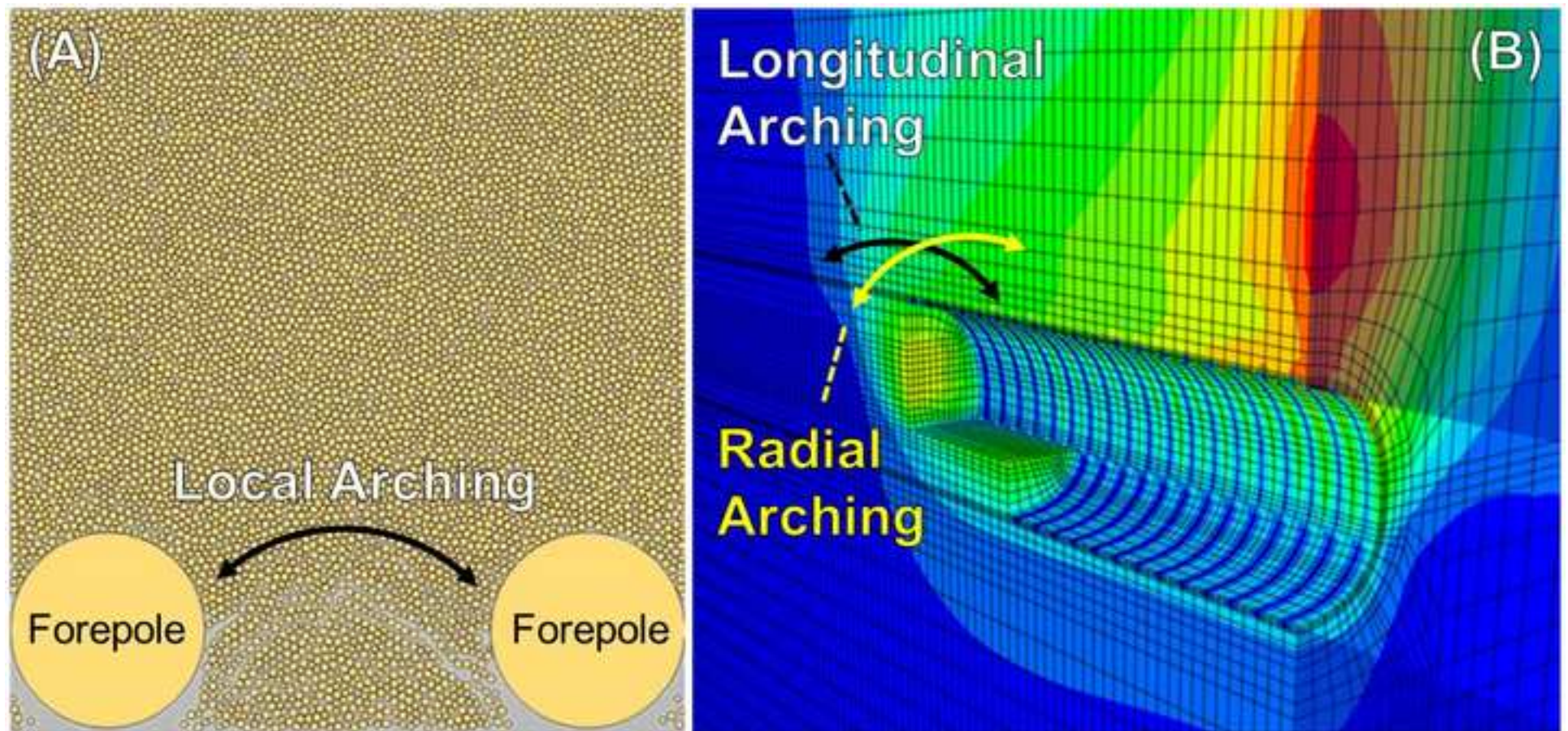
Figure4
Click here to download high resolution image

Figure5
Click here to download high resolution image

δ_{sNS} = Surface settlement with Normal Support $\delta_{sNS+UA} = \delta_{sNS}$ with addition of Umbrella Arch

$$R_{ss} = \frac{(\delta_{sNS} - \delta_{sNS+UA})}{\delta_{sNS}}$$

FpGdcUA

FpGcUA

GcUA

FpdGUA

FpGUA

Weather Soil
Weather Rock

Soft Rock

Kim et al. (2005)
FpGdcUA

Reduction of Surface Settlement (Rss)

Overburden/Height of Excavation
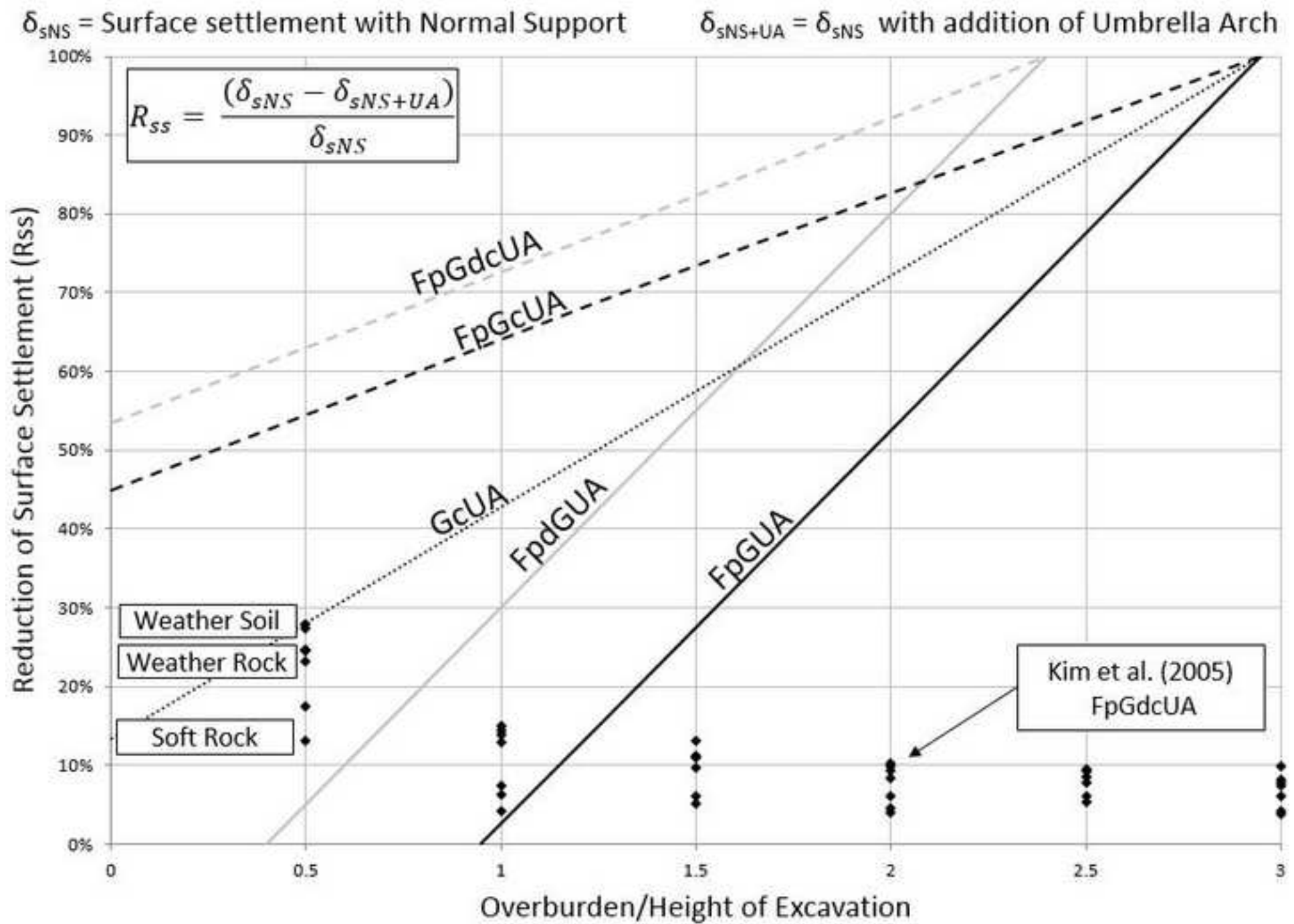
Figure6
Click here to download high resolution image
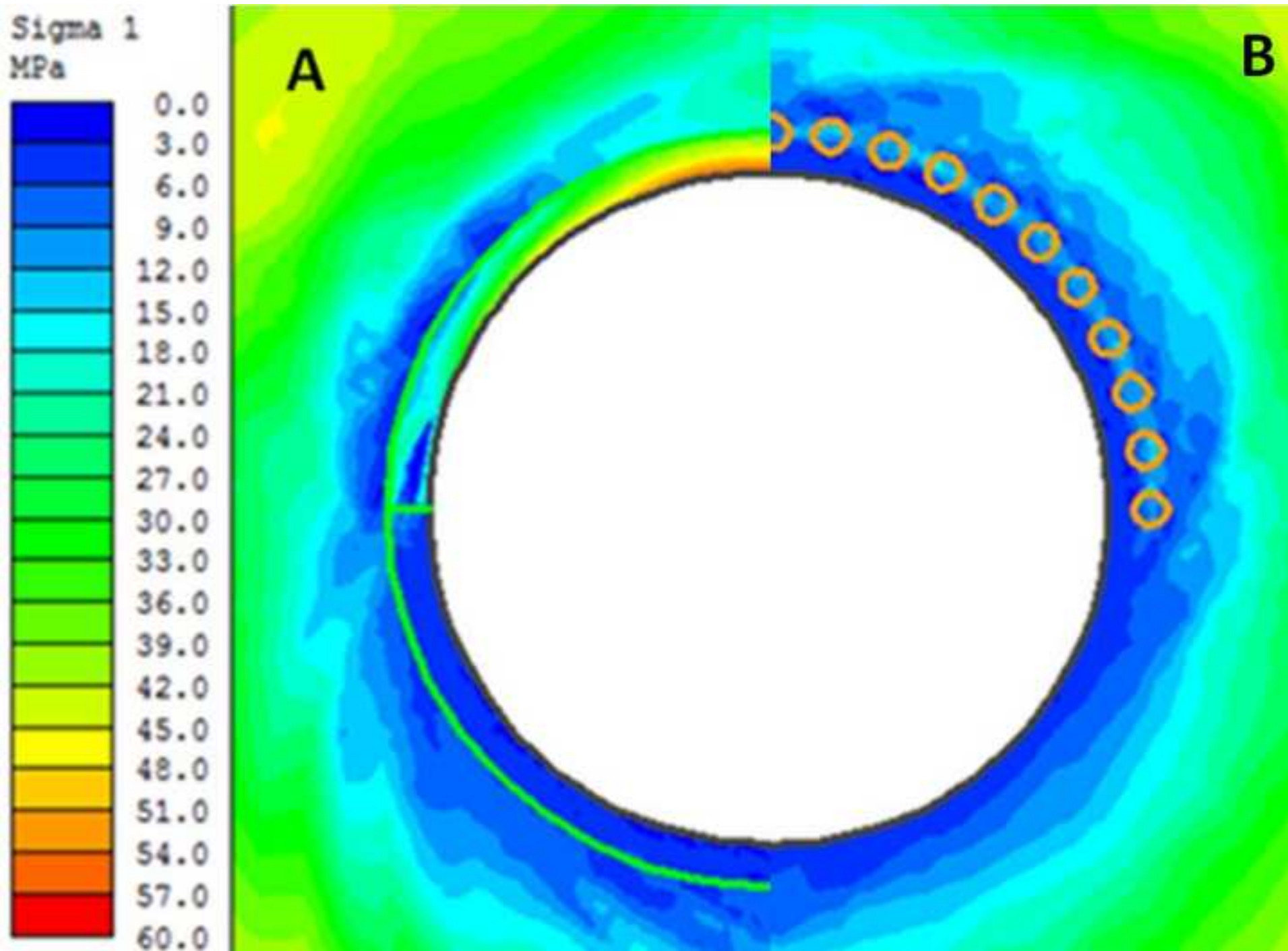
Figure7
Click here to download high resolution image

Figure 7. A) Forepole, rock mass, and excavated tunnel cross-section. B) Total Displacement (mm) vs Degrees (0 right wall, 90 invert, 180 left wall, 270 crown, and 360 right wall).
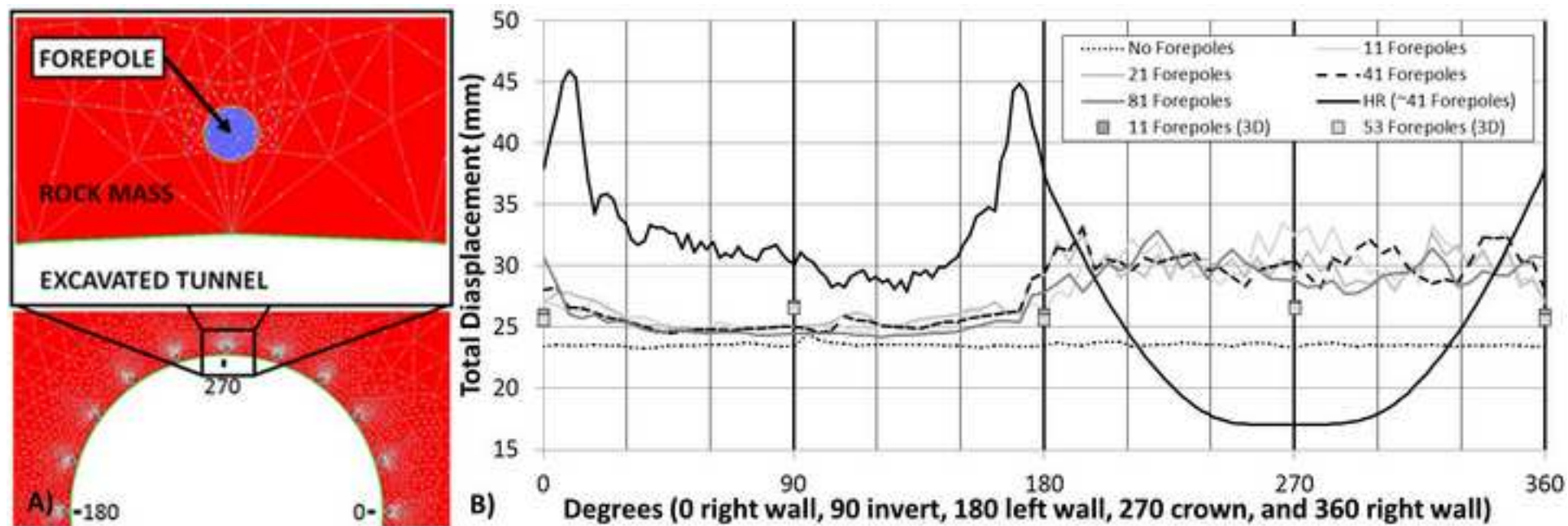
Figure8
Click here to download high resolution image

A)

B) 180m 104m

Φ=10m
Φ=22m

180m

0.25m Mesh

C) FIX X

FIX Y

FIX Z

D)

E)

Rockbolts
[Φ$_r$=19mm, L$_r$=4m, E$_r$=200GPa]

Forepoles Elements
[Φ$_{fp}$=101mm, L$_{fp}$=12m]

Shotcrete

Steel Set

Direction of Excavation

Umbrella Arch (L$_{foo}$ = 4m)

A)

B) Reinforcing Element (Steel)

Grout Annulus

Slider (Normal Cohesive Strength)

Spring (Normal Stiffness)

Axial Stiffness of Steel

Reinforcement Nodal Point

Slider (Cohesive Strength of Grout)

C) Spring (Shear Stiffness of Grout)
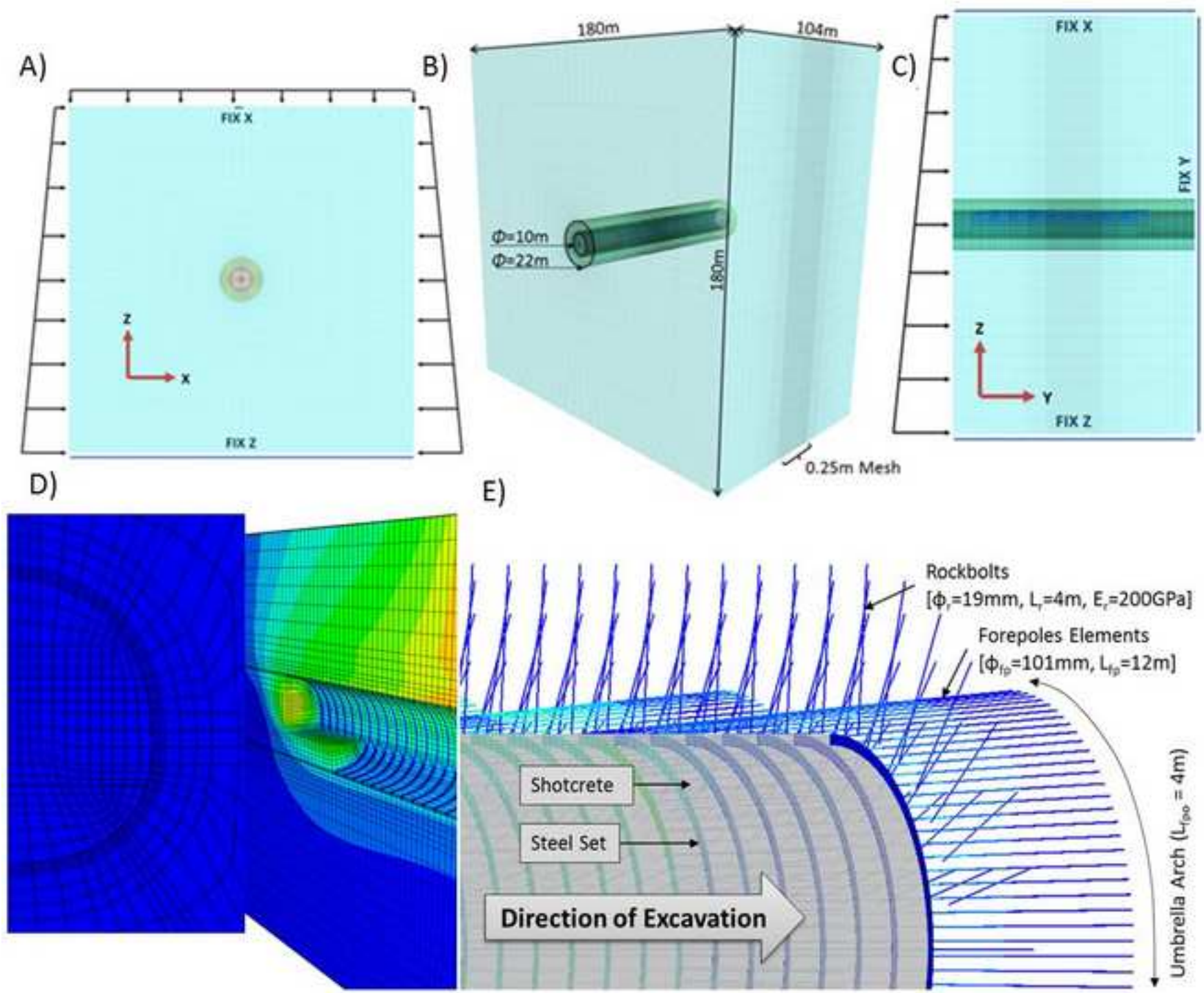
Figure10
Click here to download high resolution image
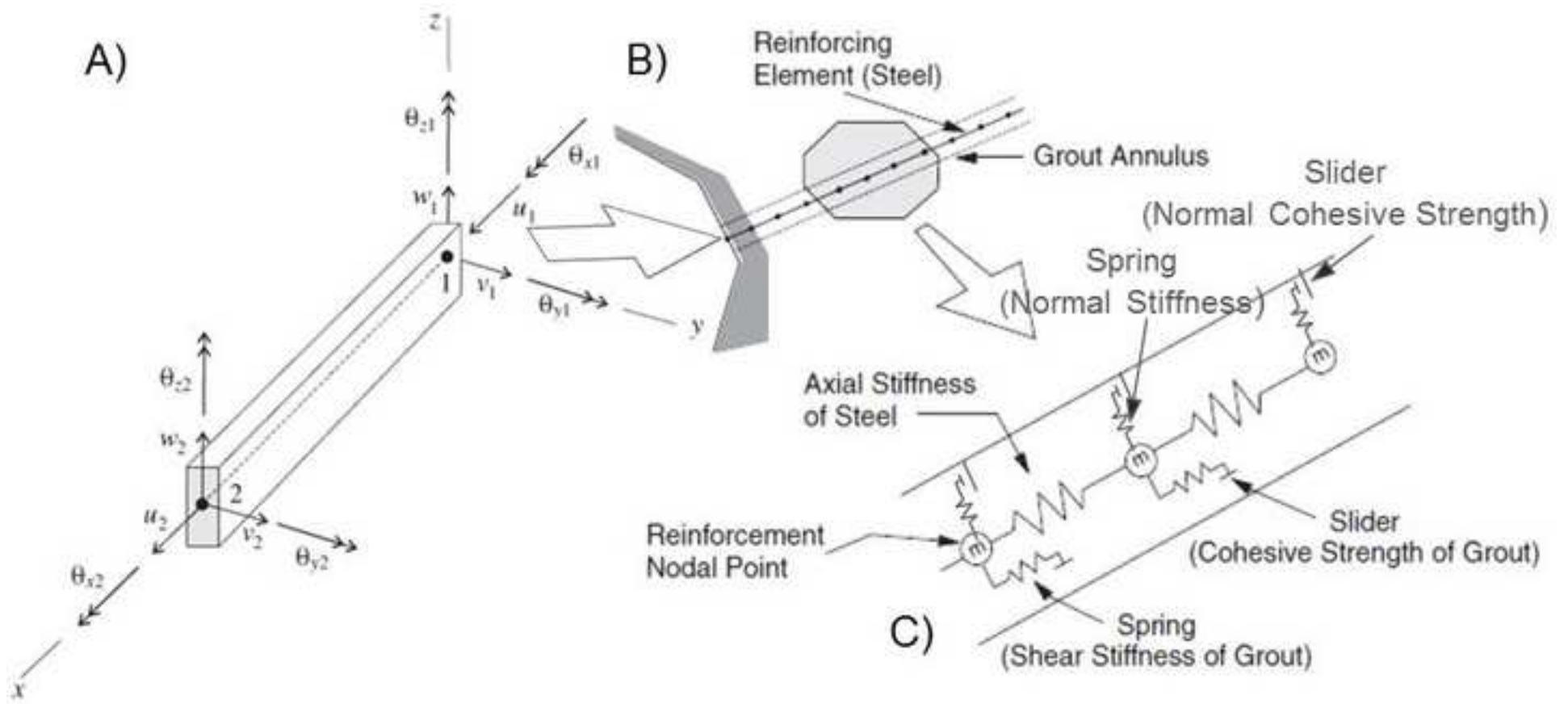
Displacement Profiles of 12m Long Forepole Elements with a 2m Overhang
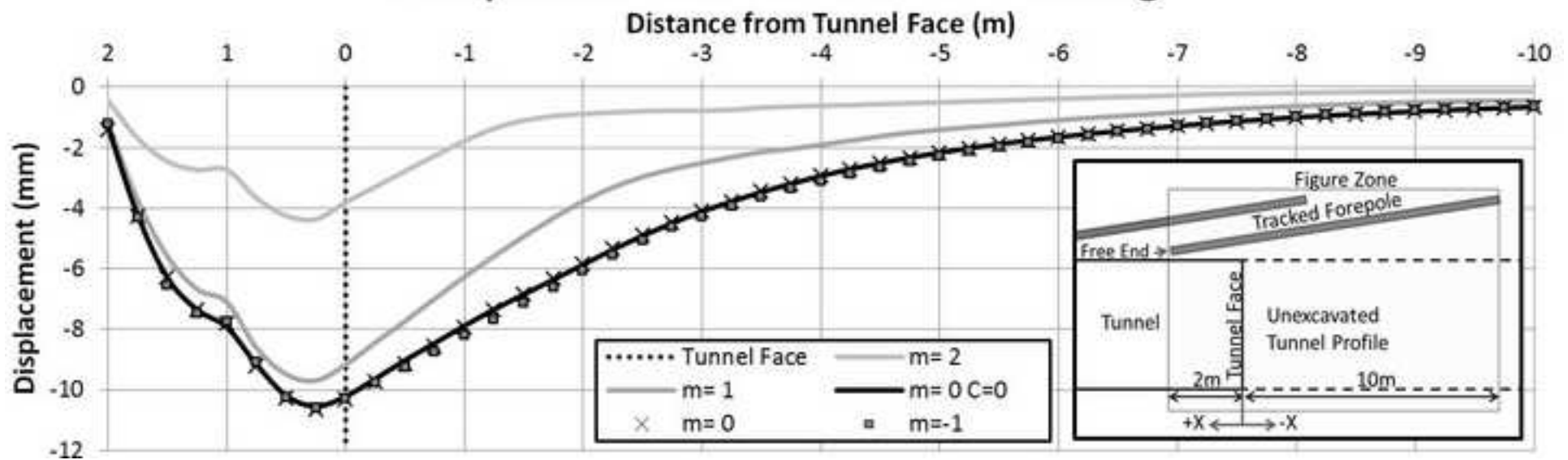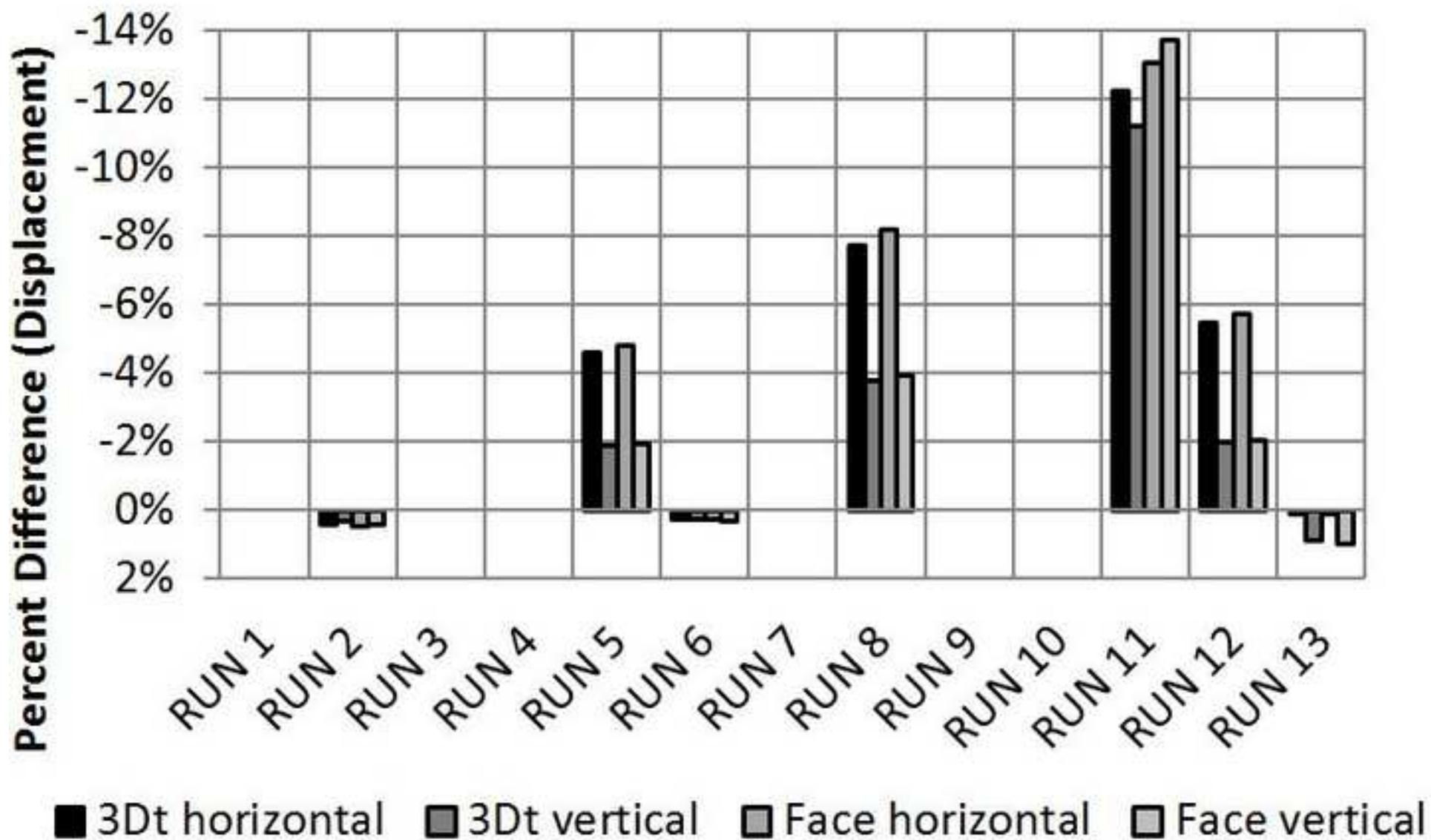
Figure11
Click here to download high resolution image

Crown Displacement

Percent Difference (Displacement)

-14%
-12%
-10%
-8%
-6%
-4%
-2%
0%
2%

RUN 1 RUN 2 RUN 3 RUN 4 RUN 5 RUN 6 RUN 7 RUN 8 RUN 9 RUN 10 RUN 11 RUN 12 RUN 13

■ 3Dt horizontal ■ 3Dt vertical ☐ Face horizontal ☐ Face vertical

Figure12
Click here to download high resolution image

Displacement Profile of First 3m of a 12m Forepole Element
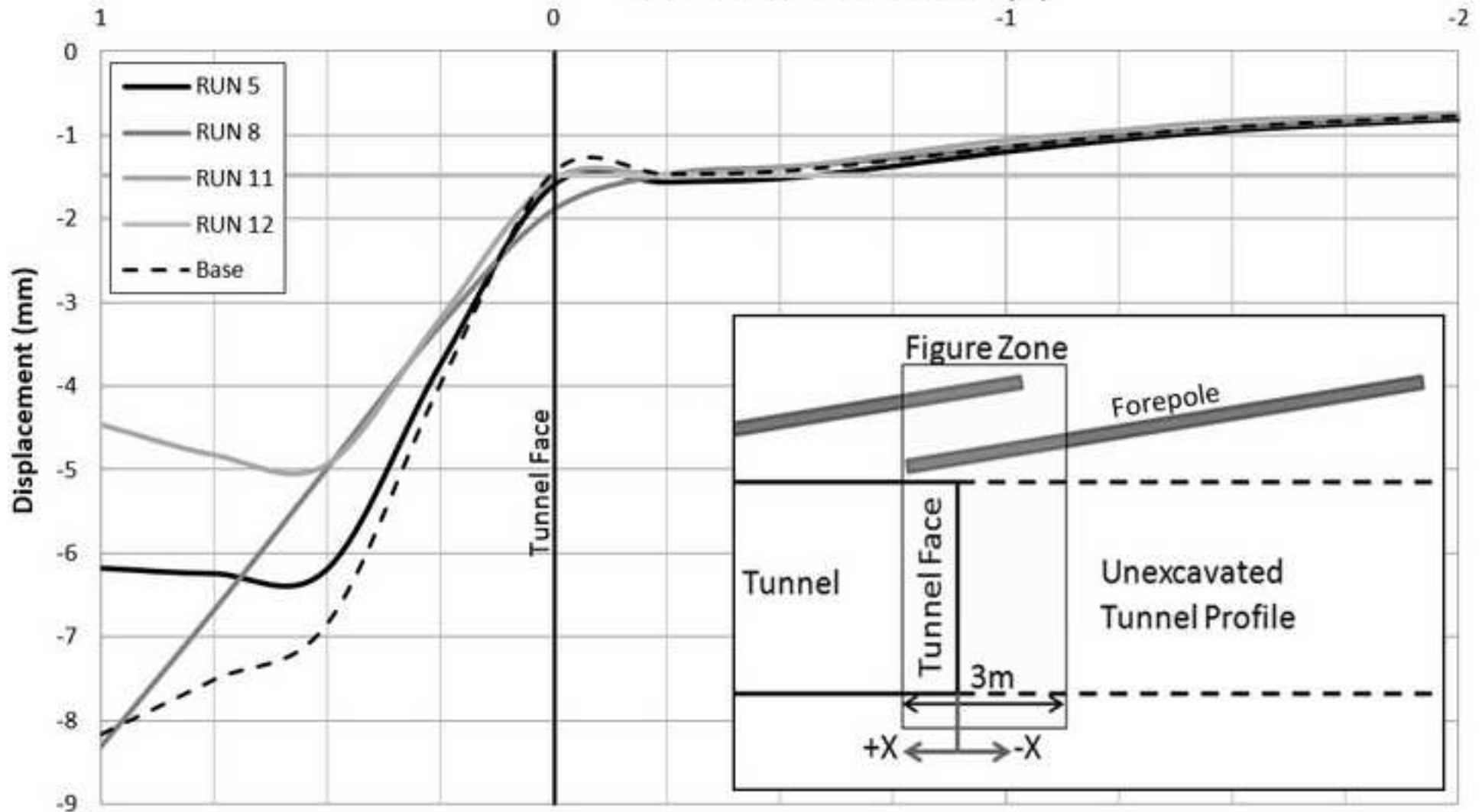
Figure13
Click here to download high resolution image
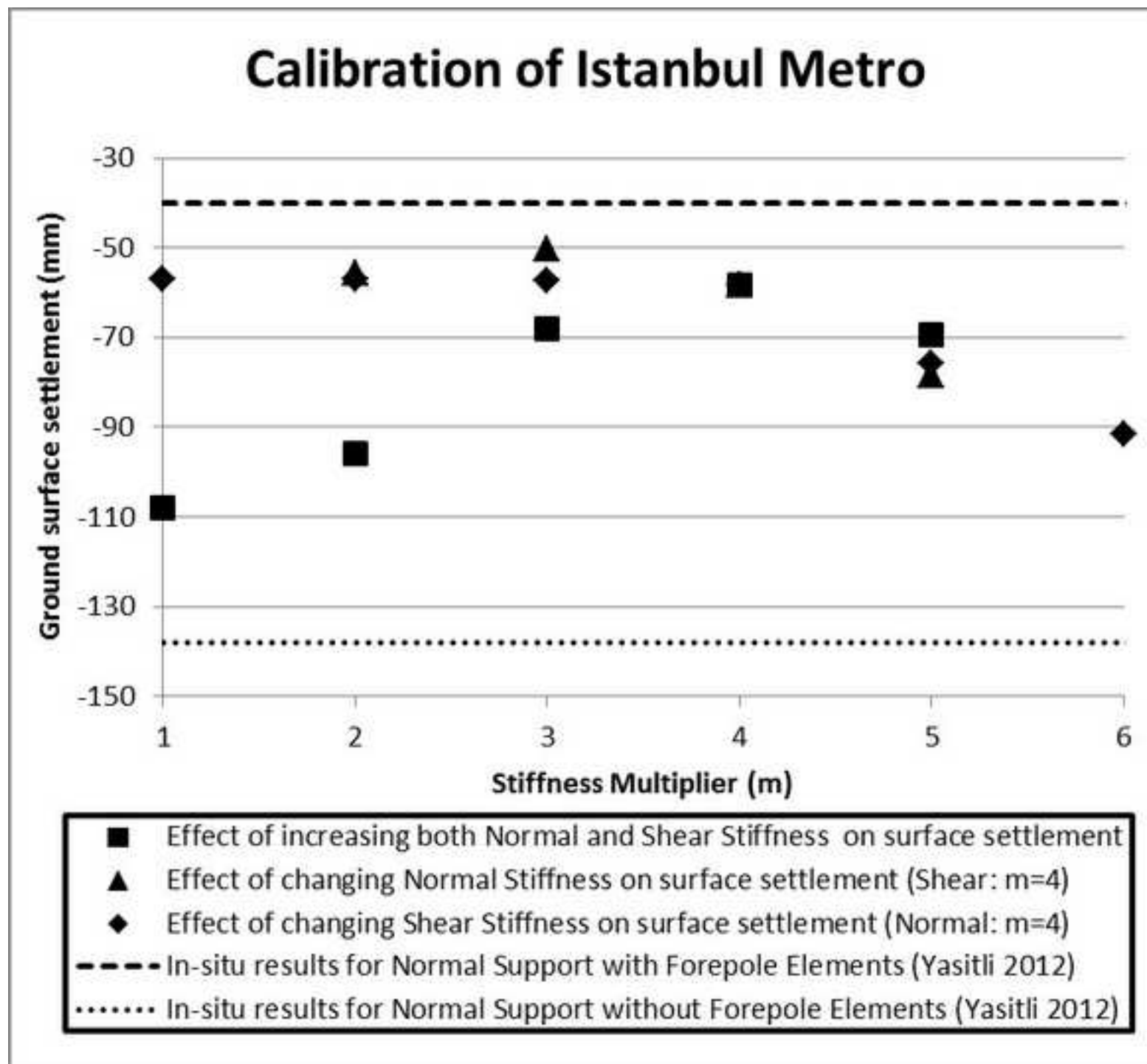
Calibration of Istanbul Metro

Displacement Profile of First 2m of a 12m Long Forepole Element

Influence of Coverage Angle and Spacing on Surface Settlement (mm)
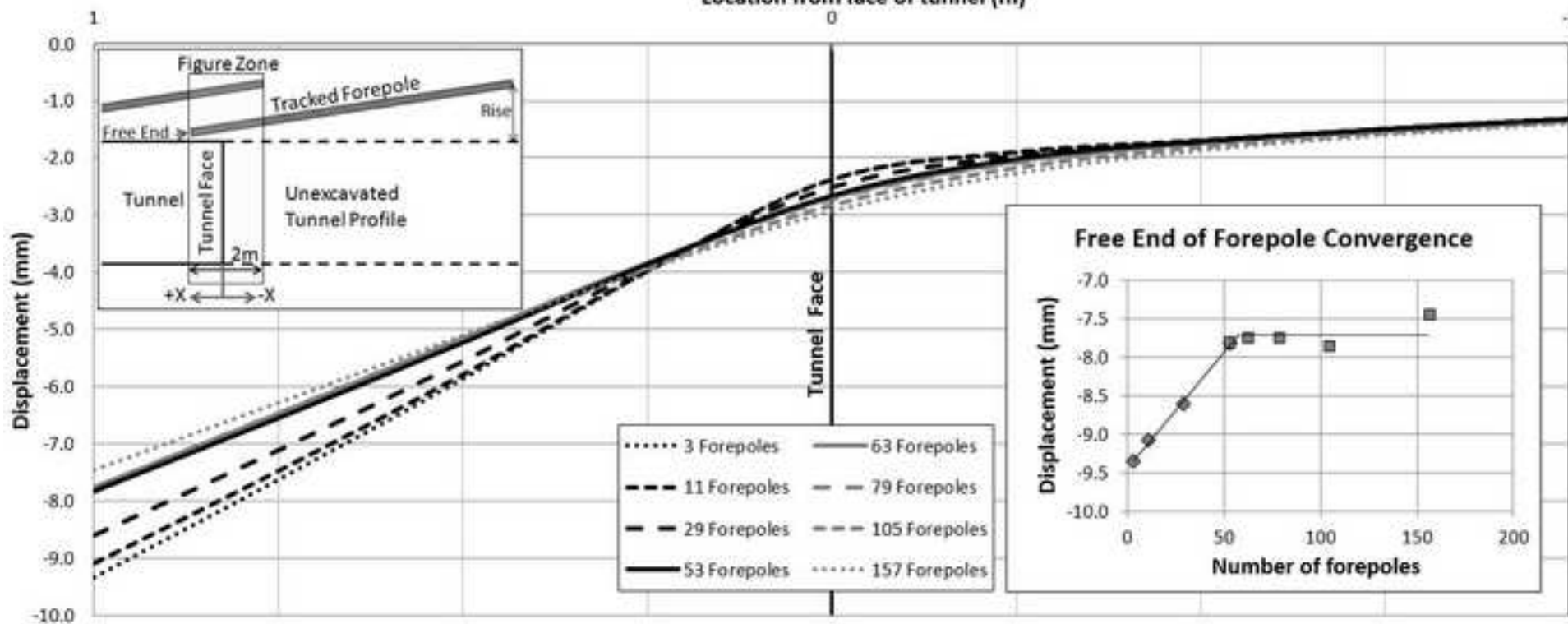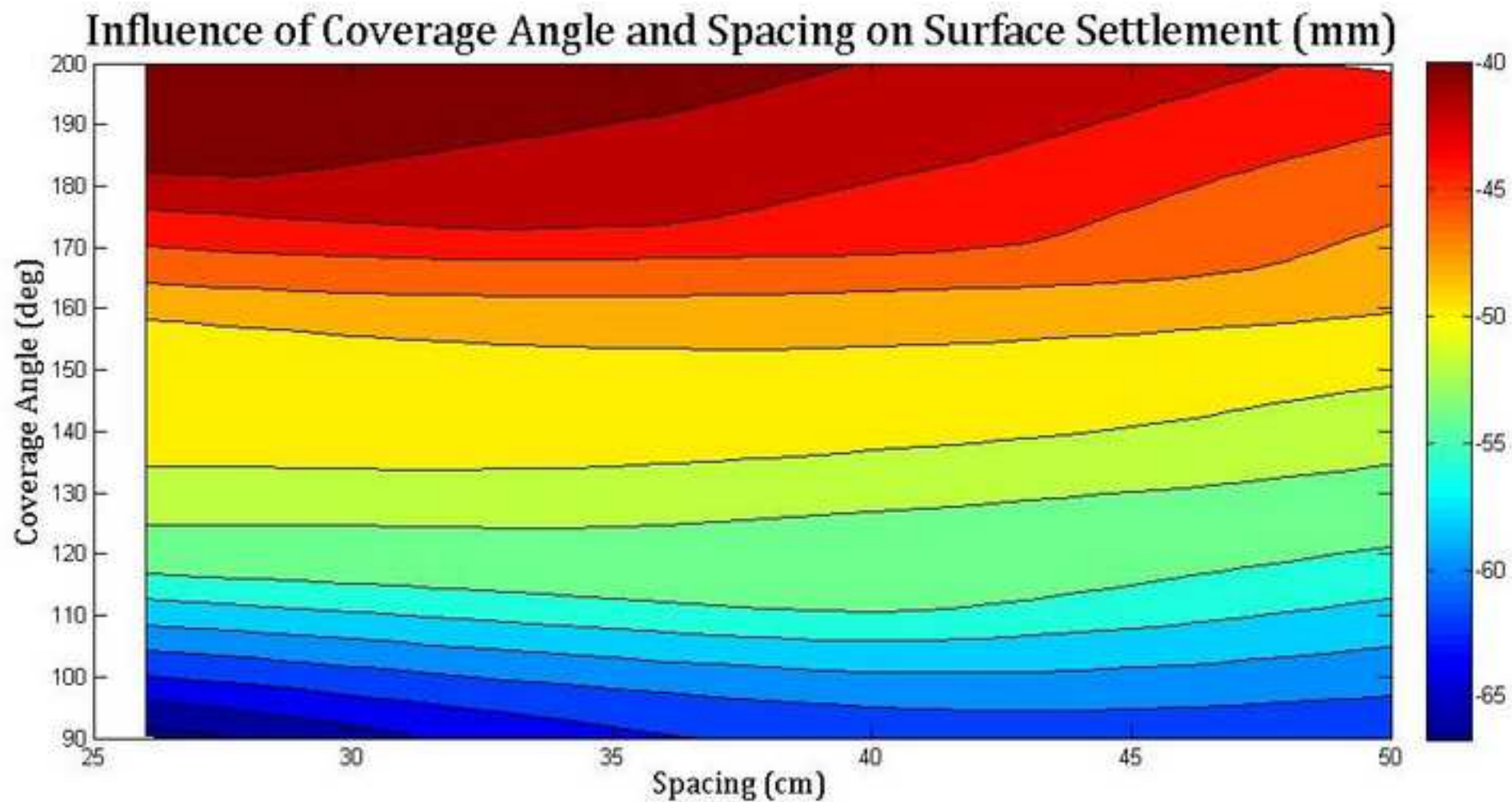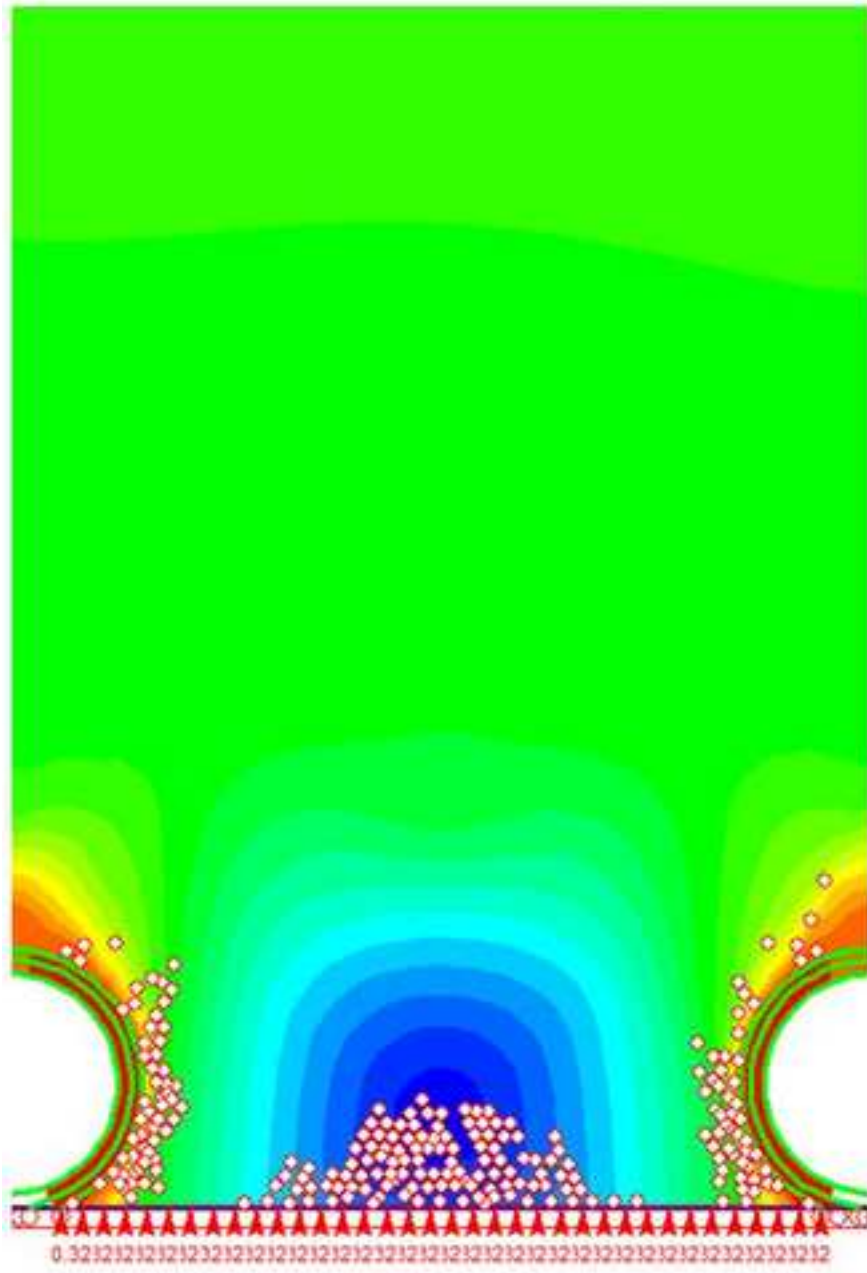
Figure16
Click here to download high resolution image

Effect of Coverage Angle on Displacement for a 40cm Forepole Spacing
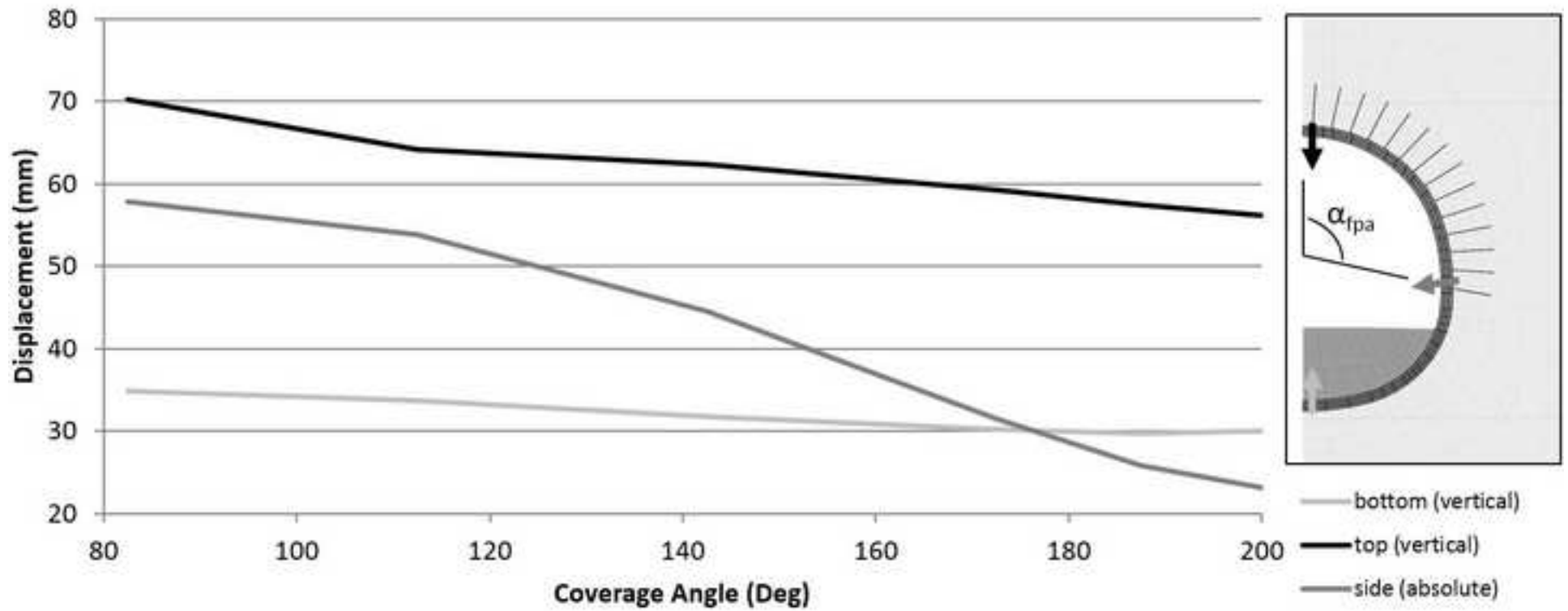
Displacement Profile of First 2m of 12m Long Forepole Element
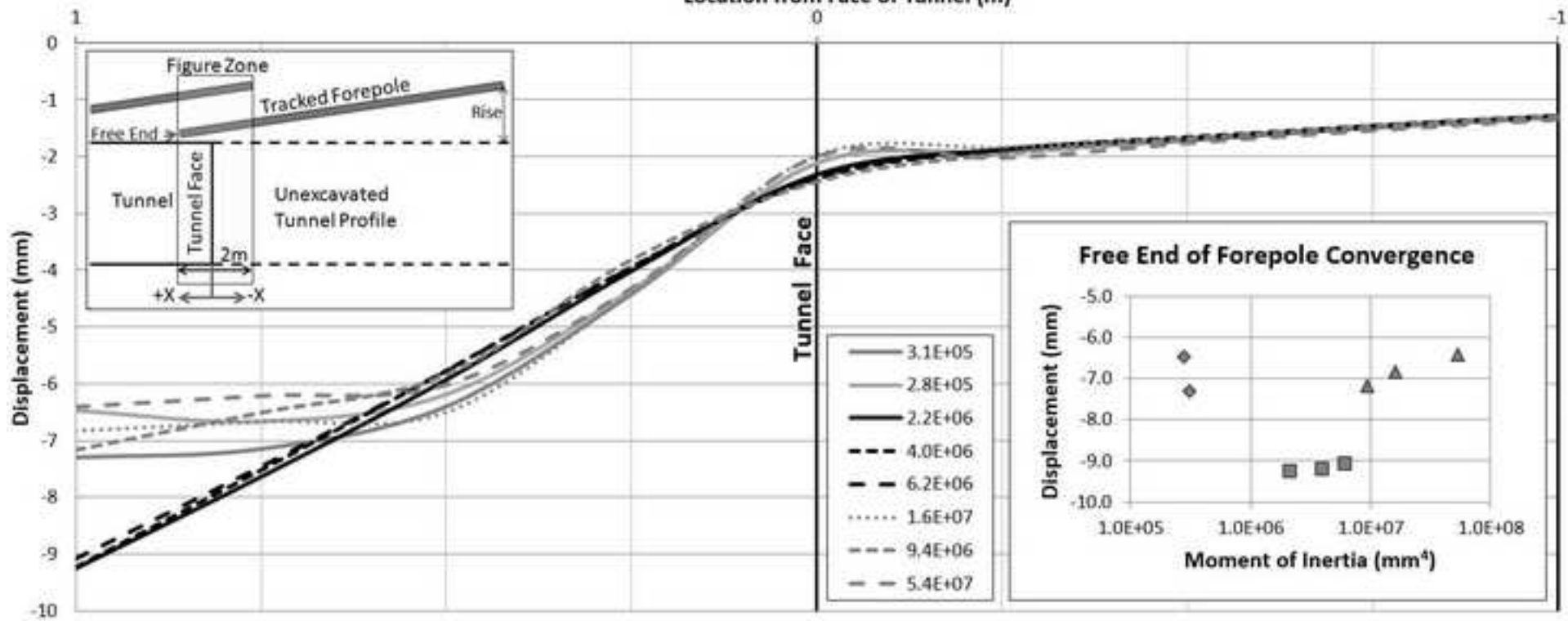
Displacement Profile of First 2m of 12m Long Forepole Element
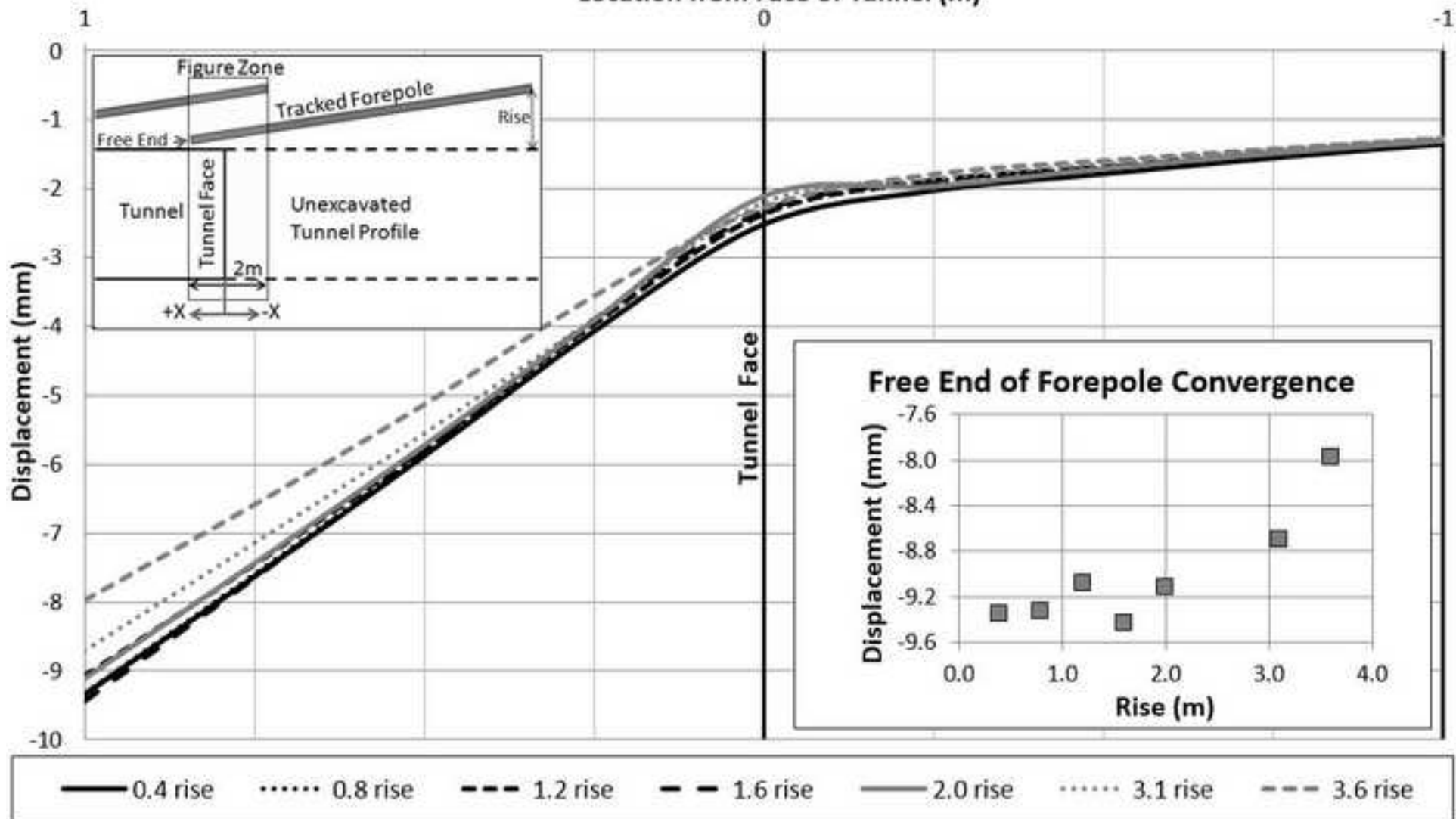
Figure19
Click here to download high resolution image
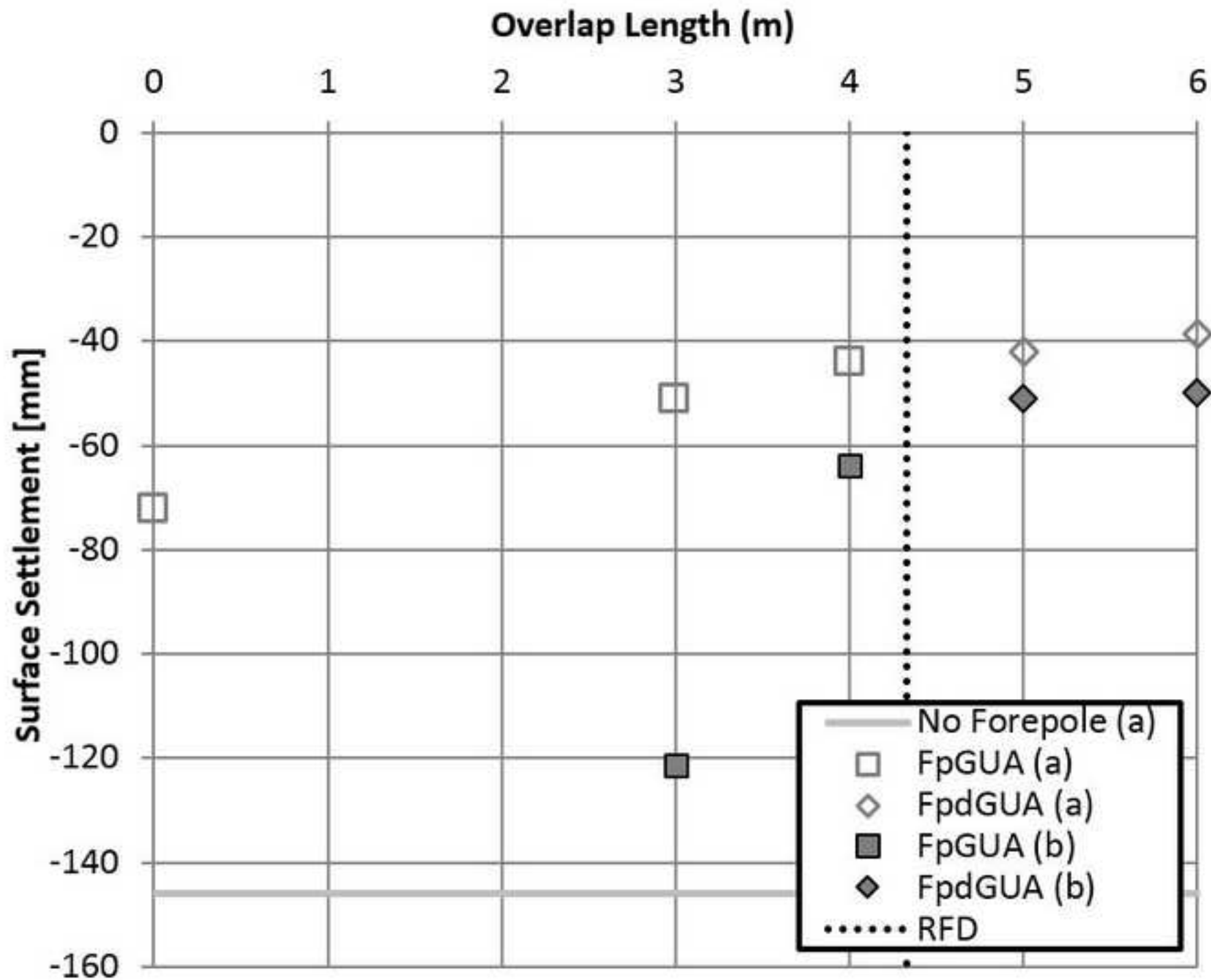
Effect of overlap of Umbrella Arches (2m Overhang)
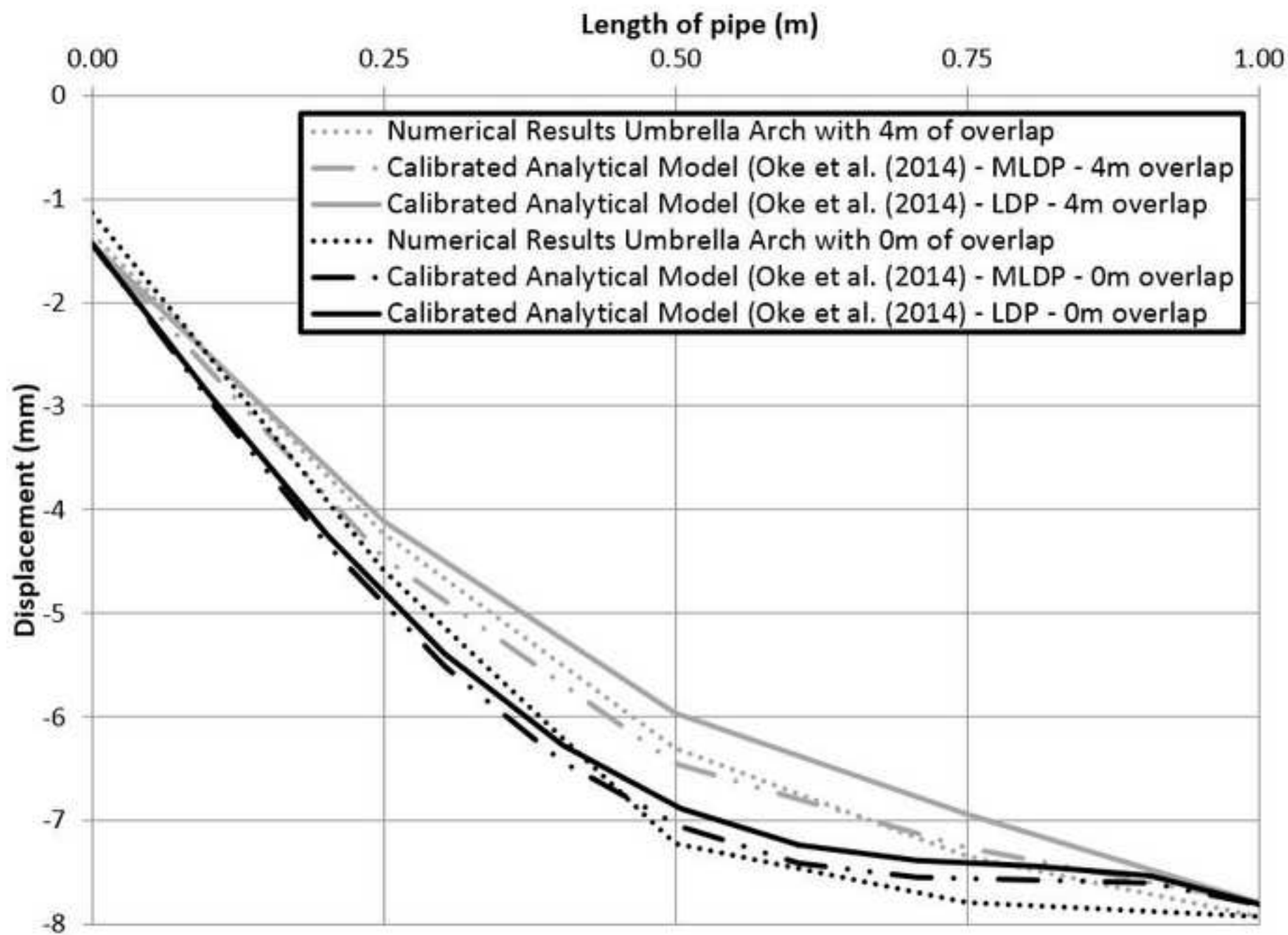
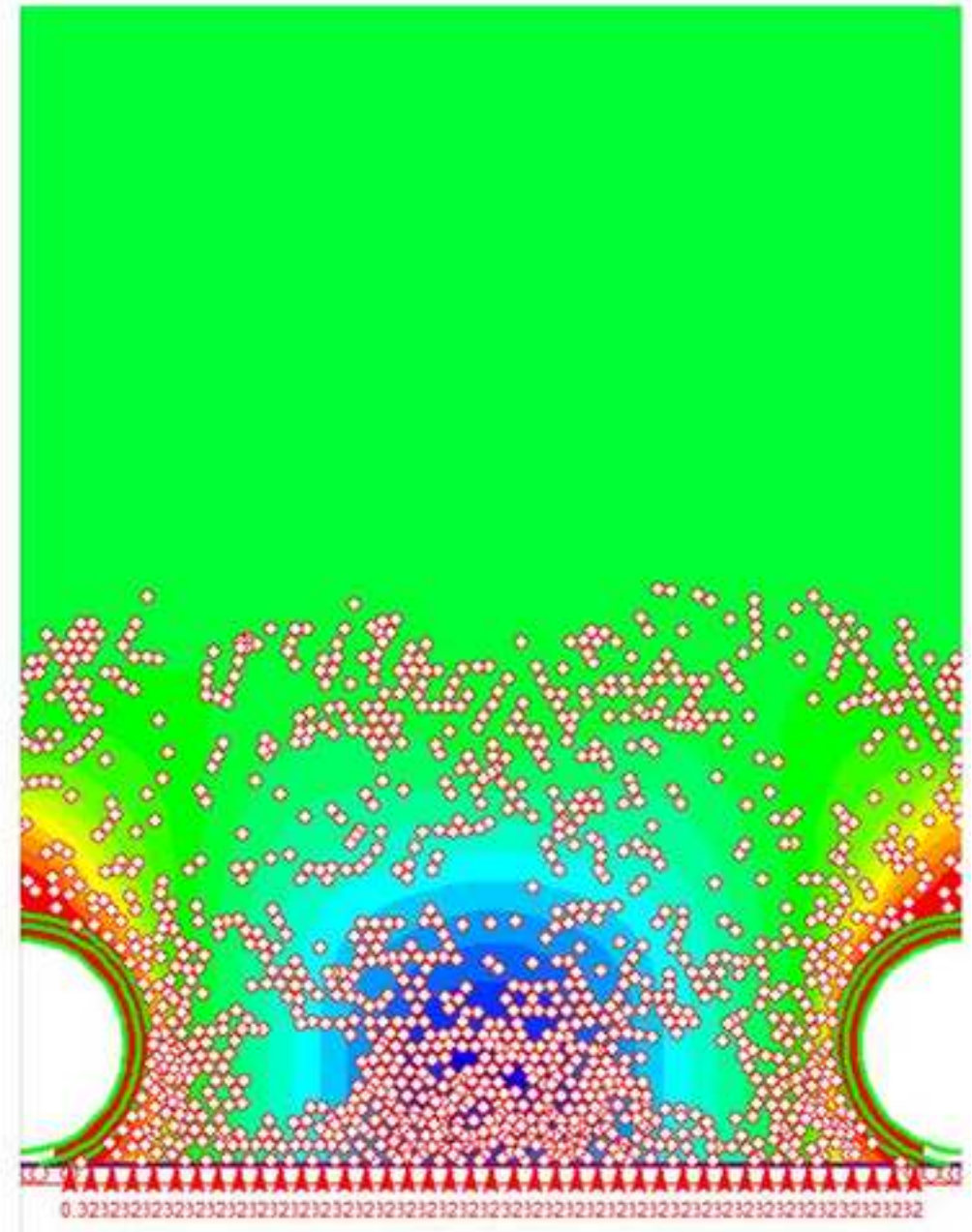**Figure21**
Click here to download high resolution image

δ_{sNS} = Surface settlement with Normal Support δ_{sNS+UA} = δ_{sNS} with addition of Umbrella Arch

Reduction of Surface Settlement (Rss)

Overburden/Height of Excavation

$$R_{ss} = \frac{(\delta_{sNS} - \delta_{sNS+UA})}{\delta_{sNS}}$$

Legend:
- FpGUA
- FpdGUA
- FpGdcUA
- FpGcUA
- GcUA

SEM (Bench without face reinforcement)
SEM (Bench with face reinforcement)
Full Face
Circular (6.5m)
Circular (6.0m)
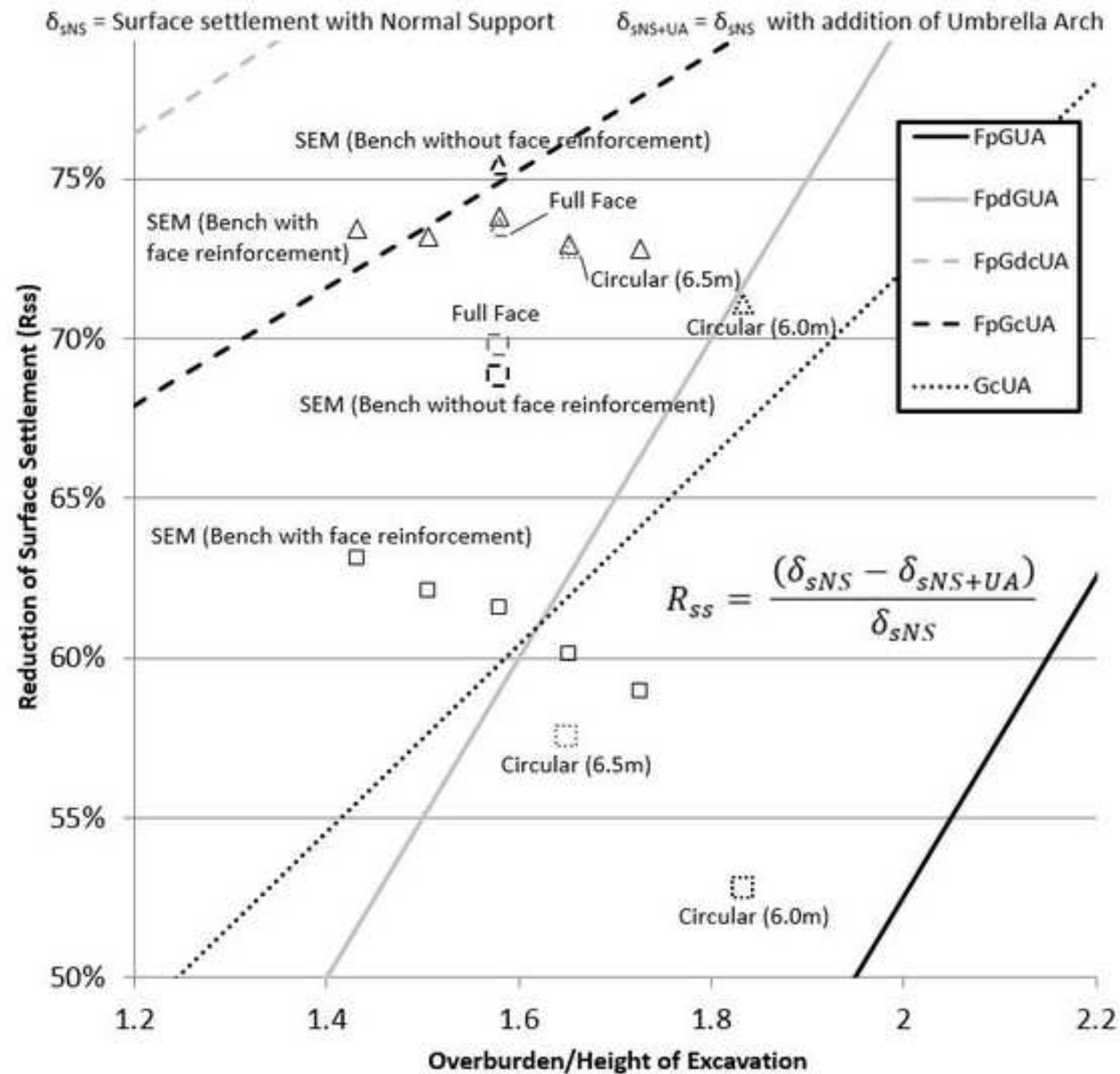
Figure22
Click here to download high resolution image
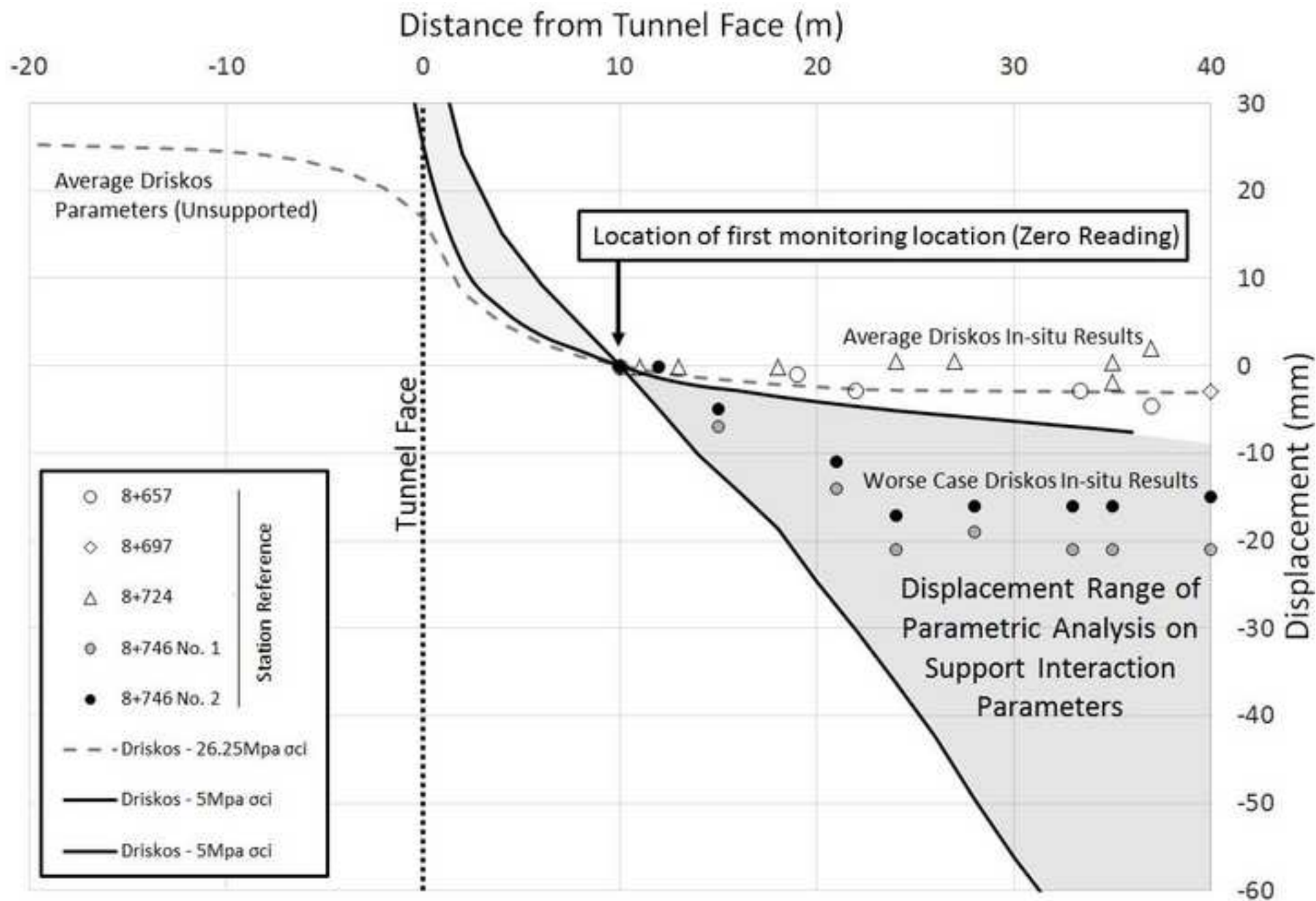
Figure22

Figure23
Click here to download high resolution image

A) Forepoles, Shotcrete + HEB Sections, Bench

B) Rockbolts, Elephant Foot

C) Forepoles, Direction of Excavation
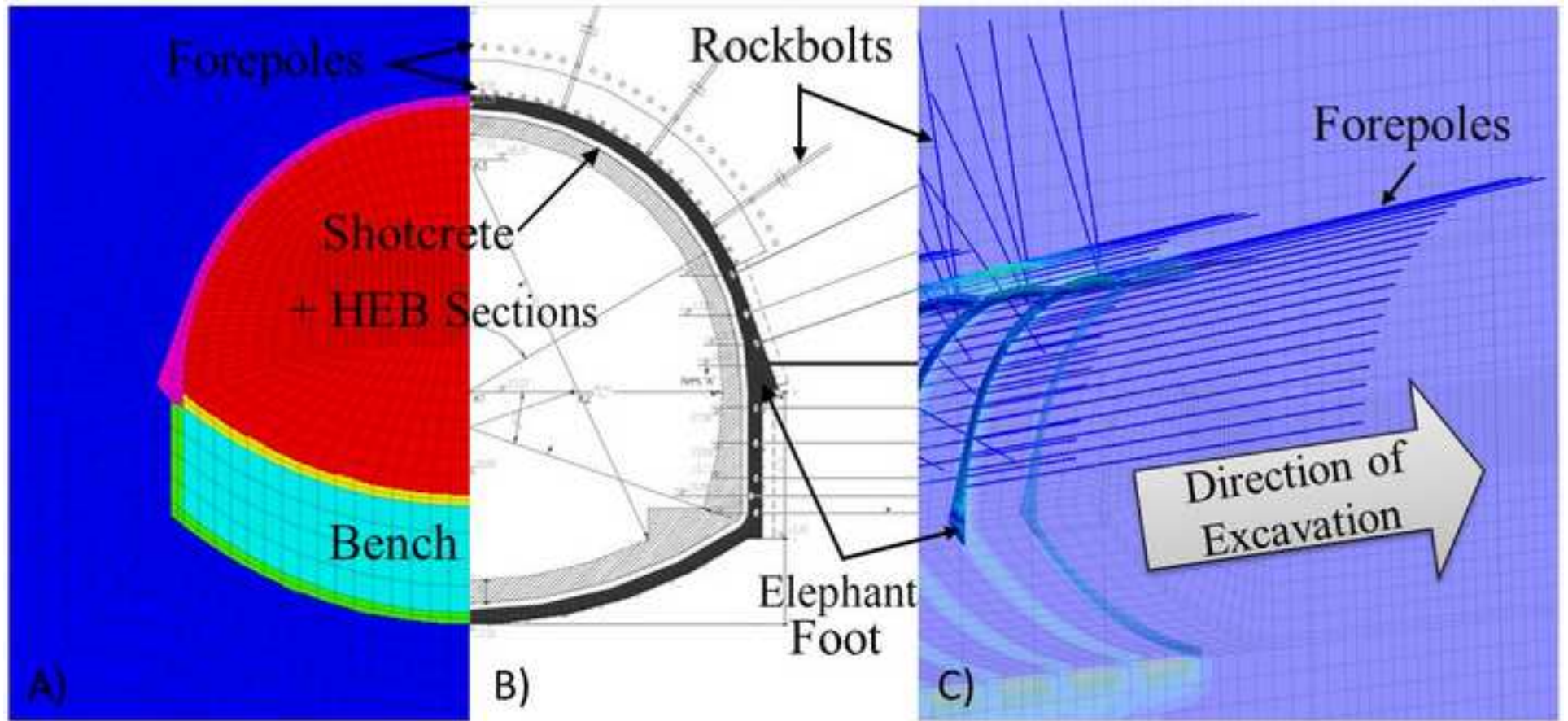
Figure24
Click here to download high resolution image
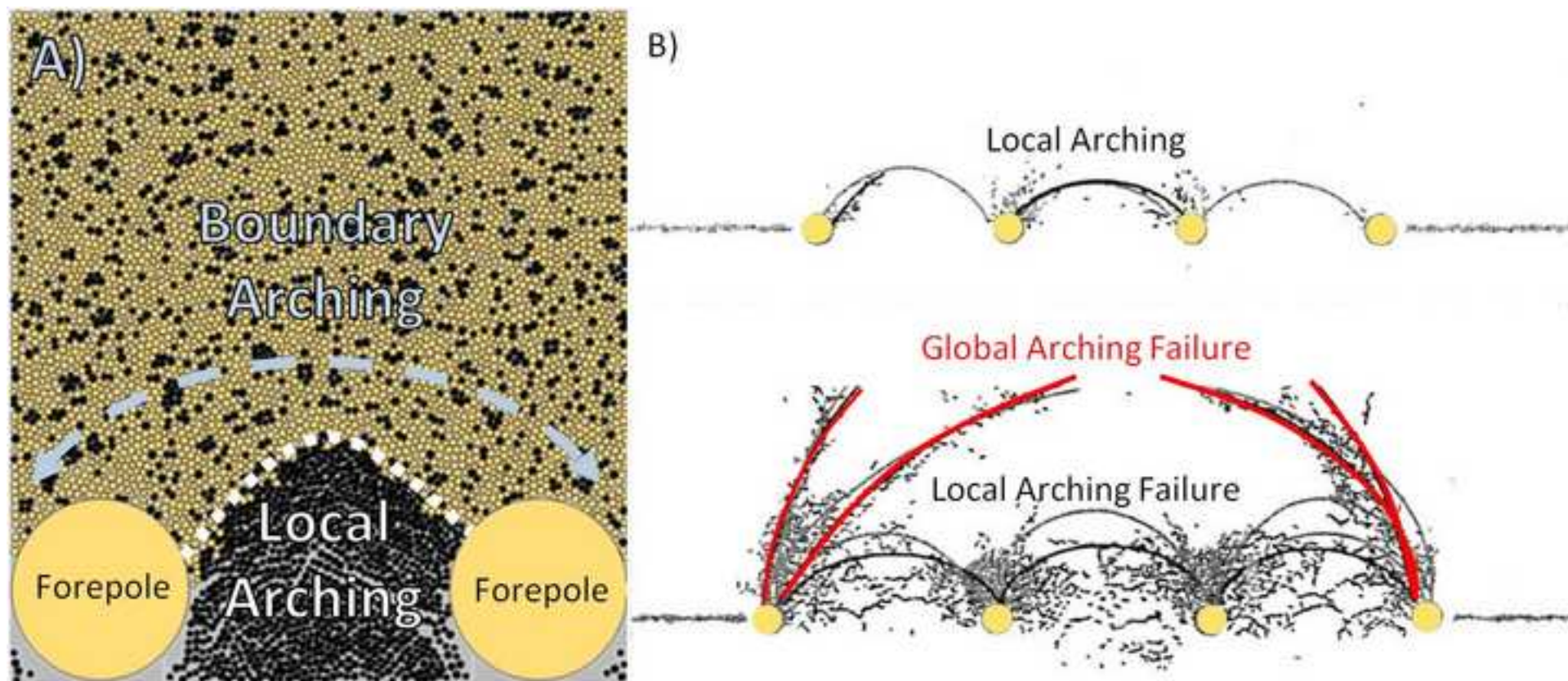
A) Boundary Arching
Local Arching
Forepole
Forepole

B) Local Arching
Global Arching Failure
Local Arching Failure

Field Stress

Gravity

0.23MPa 0.12MPa 0.01MPa 0.0Mpa

Support Stress
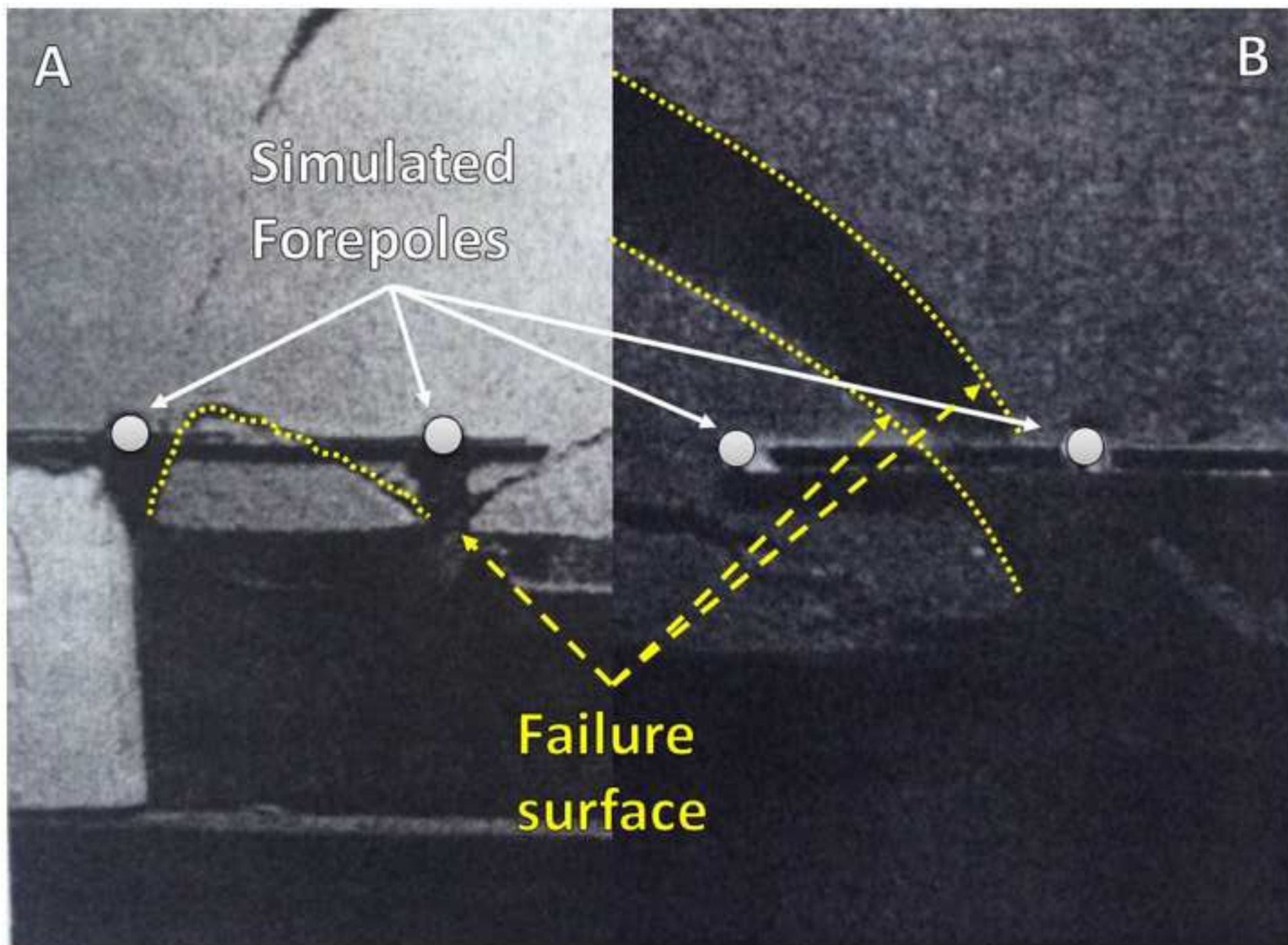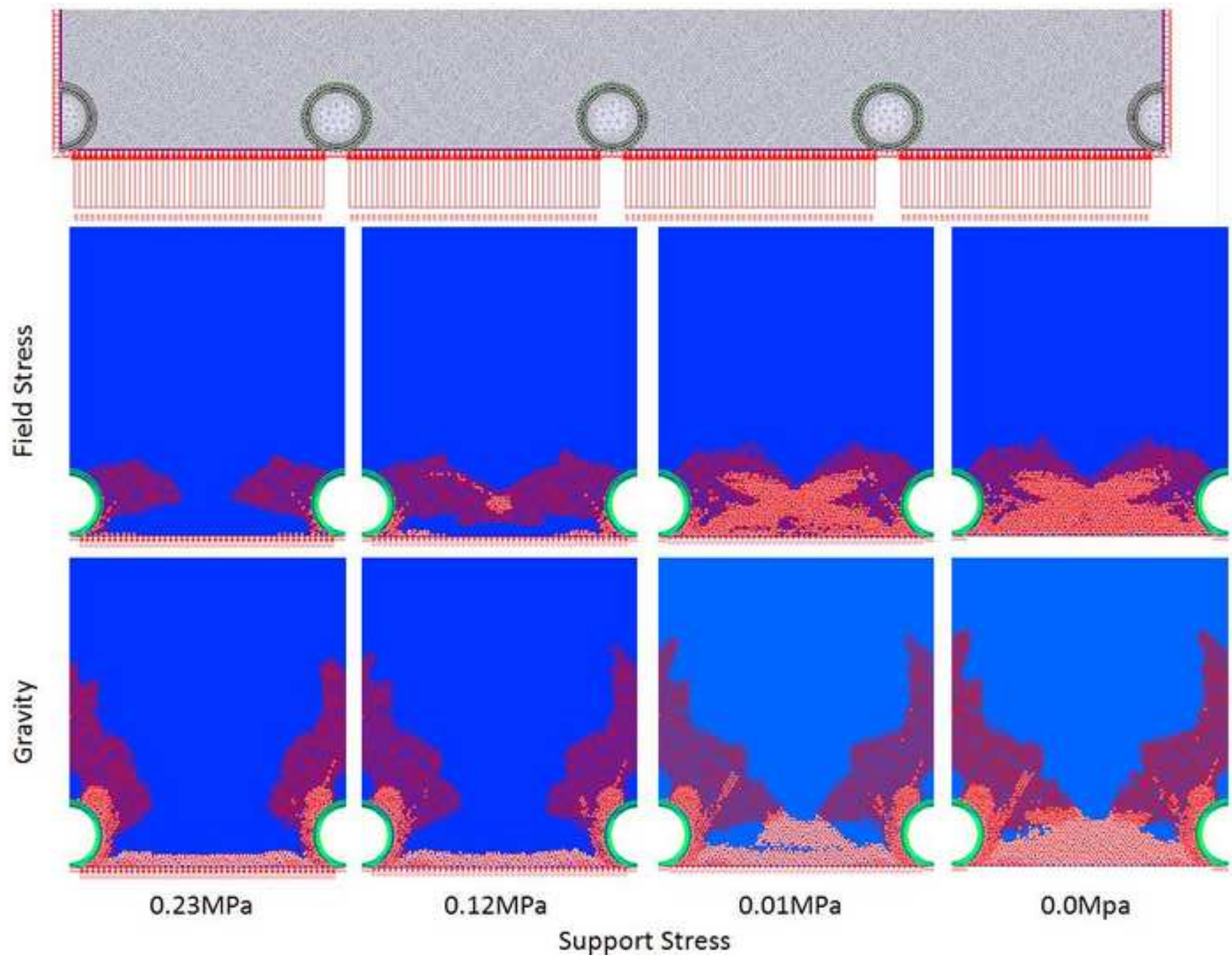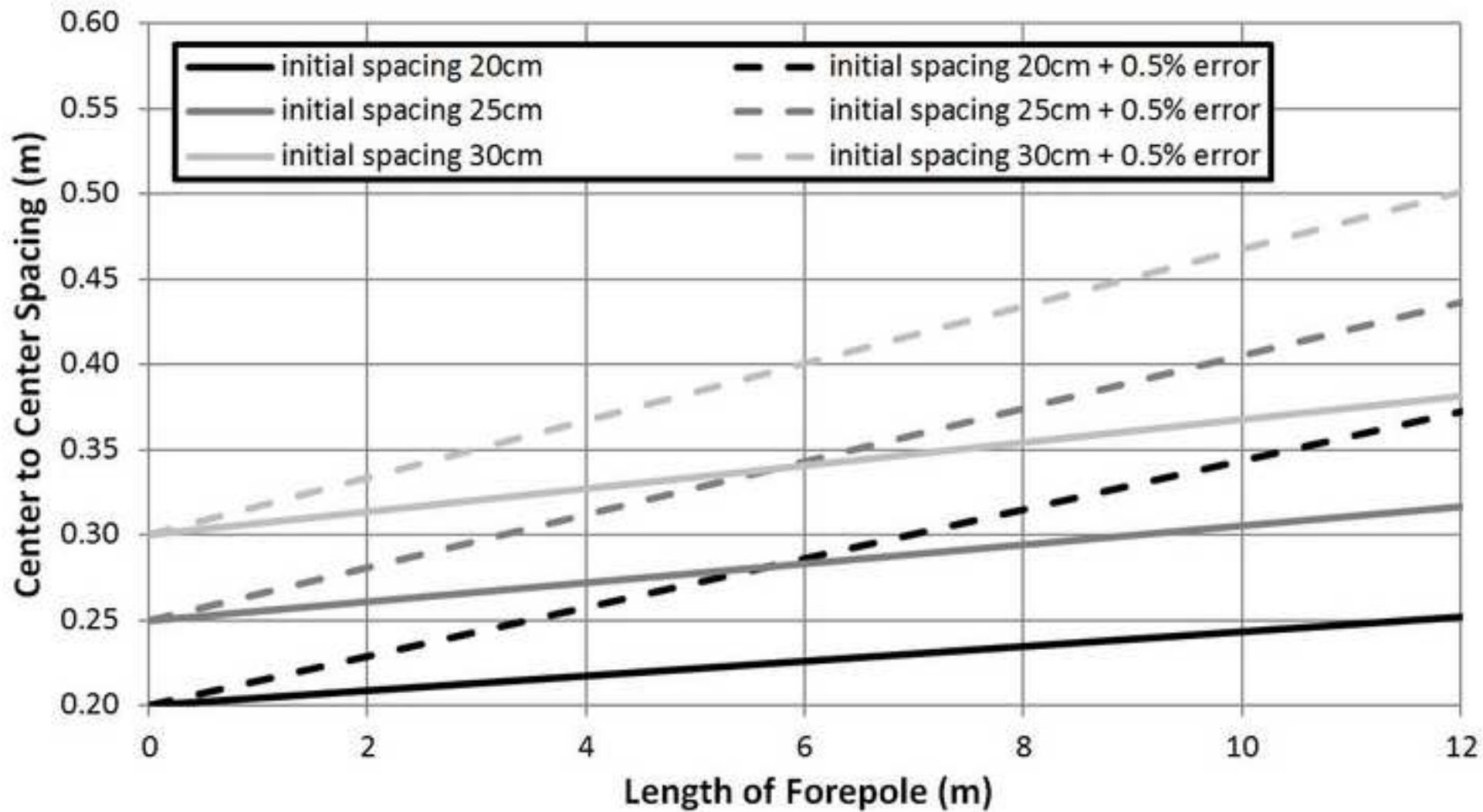
Figure28
[Click here to download high resolution image](#)

40cm

45cm
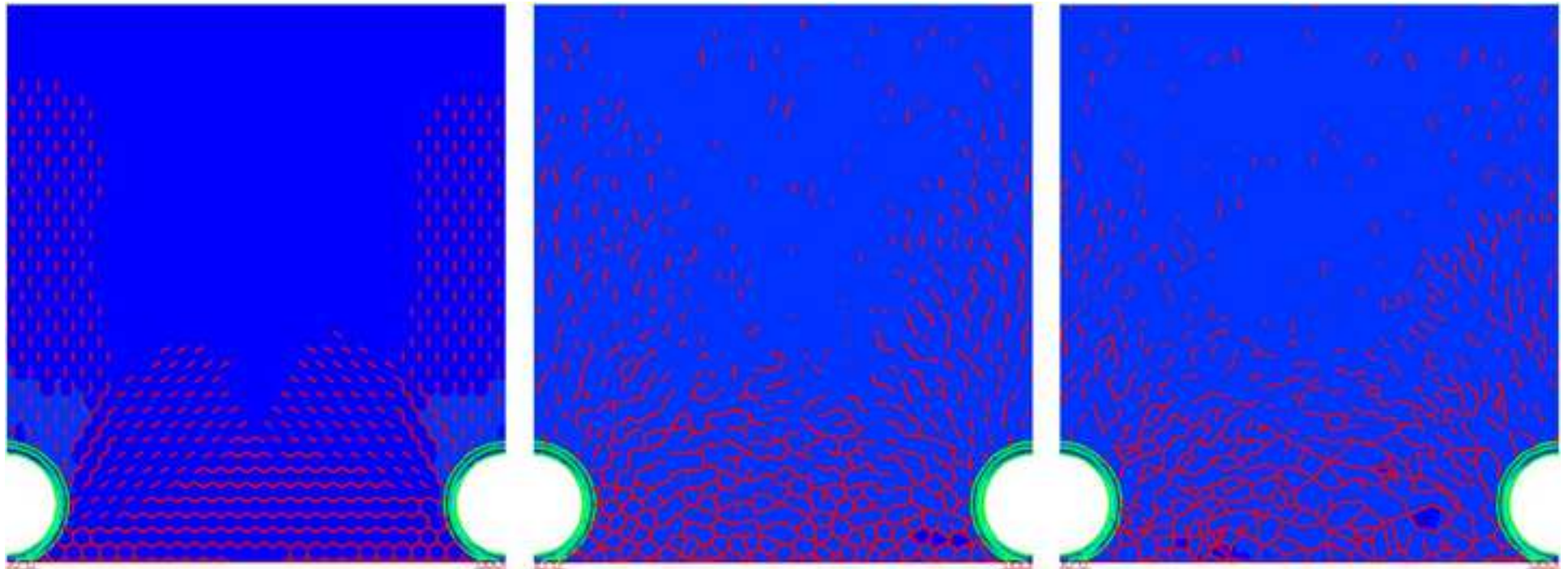
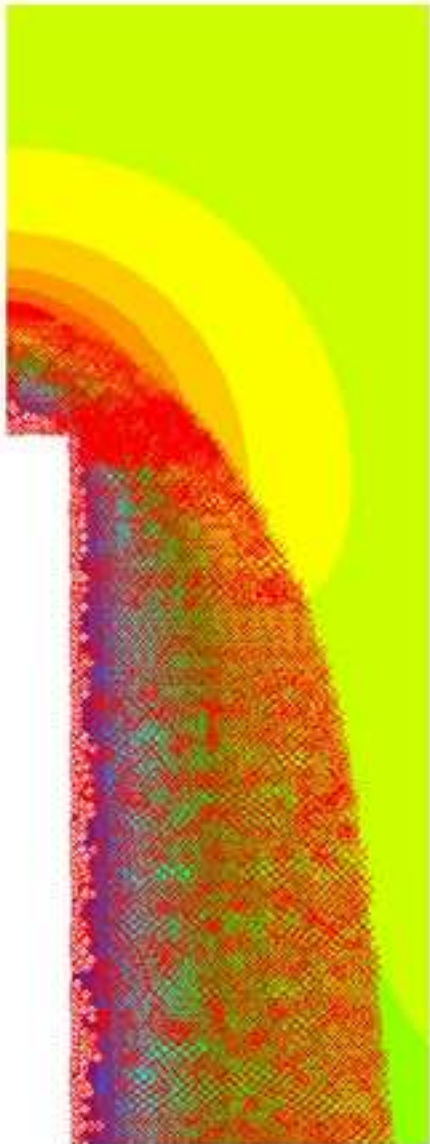Voronoi: Regular Hexagon   Voronoi: Almost Regular   Voronoi: Irregular
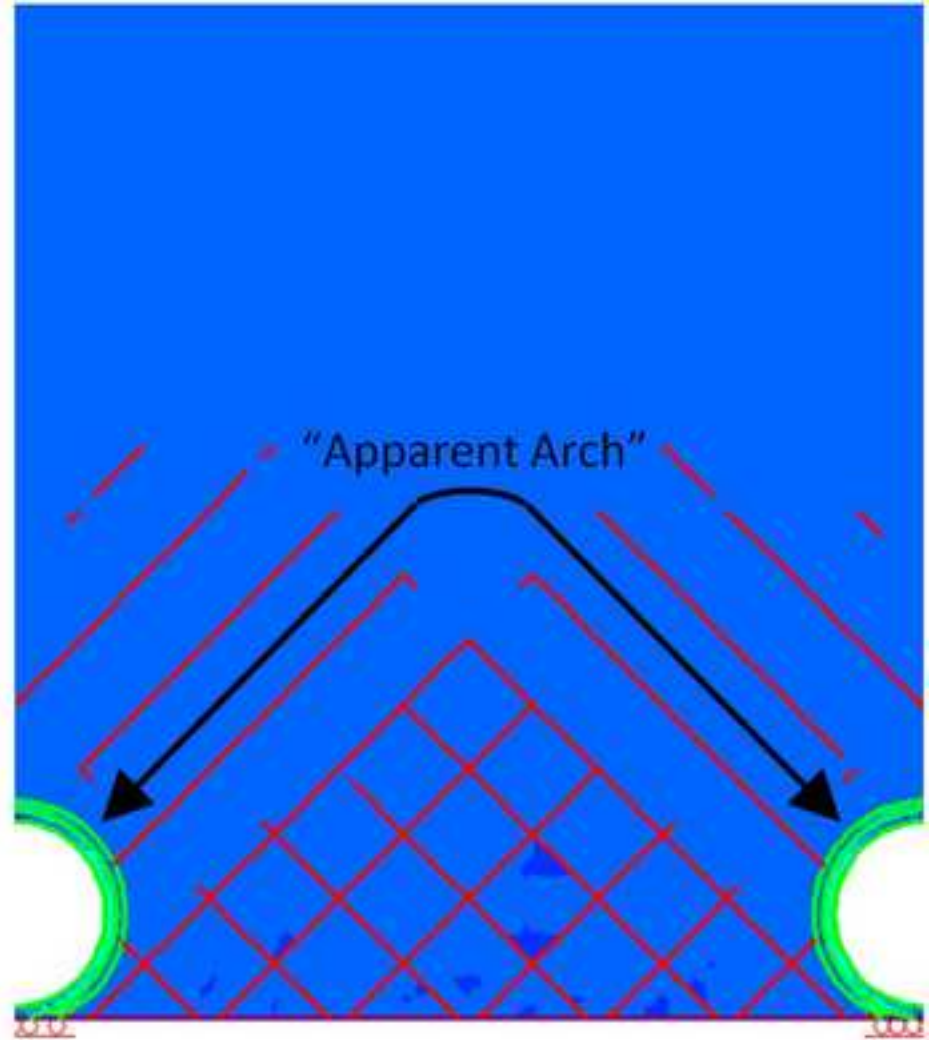
Figure30
Click here to download high resolution image

Joint 1: 90
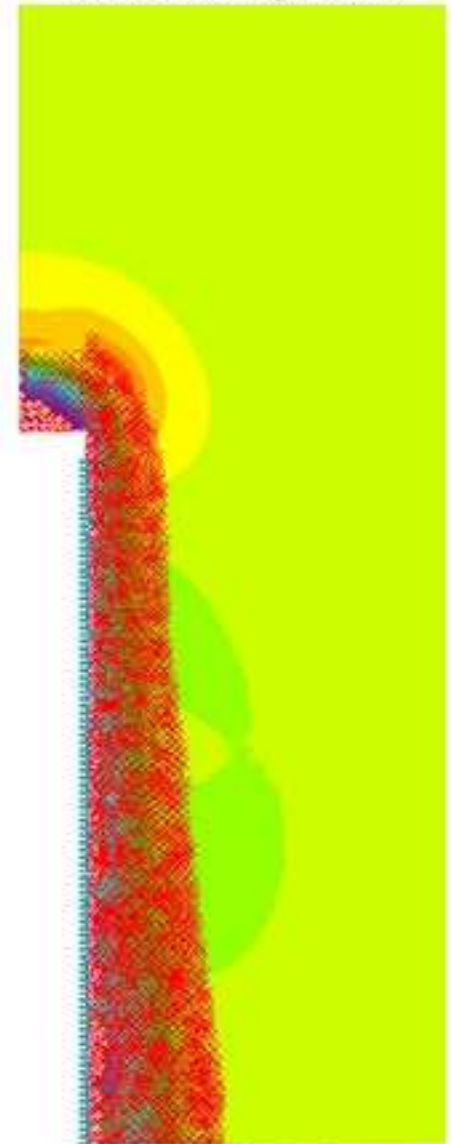Joint 2: 0

Joint 1: 45
Joint 2: -45

Unsupported — Plastic: 3.496m

Supported — Plastic: 3.401m

Supported + Face Pressure — Plastic: 3.112m

Supported + Core Material Improved — Plastic: 3.112m

Figure32